Silencing hsa_circ_0049271 attenuates hypoxia-reoxygenation (H/R)-induced myocardial cell injury via the miR-17-3p/FZD4 signaling axis

Huocheng Liao[1,2], Chun Xiao[2], Weiwei Li[2], Wenzhong Chen[2], Dingcheng Xiang[1,3]

[1]School of Clinical Medicine, Southern Medical University (PLA Southern Theater General Hospital), Guangzhou, China; [2]Cardiovascular Medicine, Huizhou Third People's Hospital, Huizhou, China; [3]Cardiovascular Medicine, General Hospital of Southern Theatre Command of PLA, Guangzhou, China

Contributions: (I) Conception and design: H Liao, D Xiang; (II) Administrative support: C Xiao; (III) Provision of study materials or patients: W Li; (IV) Collection and assembly of data: W Chen; (V) Data analysis and interpretation: D Xiang, H Liao; (VI) Manuscript writing: All authors; (VII) Final approval of manuscript: All authors.

Correspondence to: Dingcheng Xiang. Southern Medical University, Guangzhou, China. Email: dcxiang@foxmail.com.

Background: This study sought to explore the role and molecular mechanism of circ_0049271 in hypoxia-reoxygenation (H/R)-induced cardiomyocyte injury.

Methods: Significantly upregulated circular ribonucleic acids (circRNAs) in Gene Expression Omnibus (GEO) data sets were identified using a Venn diagram. A H9c2 (rat cardiomyocytes) cell model of acute myocardial infarction (AMI) was induced by 1% H/R. Quantitative reverse transcription-polymerase chain reaction was used to detect the expression levels of circ_0049271, miR-17-3p, and FZD4 in clinical blood samples and cells, and Cell Counting Kit-8 (CCK-8) was used to determine the proliferation rate of the cells in each group. Next, flow cytometry and Western blot were used to evaluate cell apoptosis. Biochemical tests and enzyme-linked immunosorbent assays (ELISAs) were then used to determine the activities/levels of the cell damage markers [i.e., creatine kinase (CK) and lactate dehydrogenase (LDH)], oxidative stress substances [i.e., malondialdehyde (MDA), reactive oxygen species (ROS), and superoxide dismutase (SOD)], and inflammatory factors [i.e., interleukin (IL)-1β, IL-6, and IL-8]. In addition, intermolecular interactions were verified using dual-luciferase reporter and RNA pull-down experiments.

Results: Circ_0049271 was significantly upregulated in both the blood of the AMI patients and the H/R-induced H9c2 cells. The knockdown of circ_0049271 increased the cell proliferation rate, decreased the apoptosis rate, inhibited oxidative stress (ROS and MDA were upregulated, and SOD was downregulated) and inflammatory responses (IL-1, IL-6, and IL-8 were downregulated), and relieved cell damage. However, the overexpression of circ_0049271 promoted H/R-induced H9c2 cell damage. Further experiments showed that miR-17-3p was a target of circ_0049271, and miR-17-3p was negatively correlated with circ_0049271 in the AMI blood samples. Additionally, miR-17-3p was found to target FZD4. A further exploration also revealed that miR-17-3p knockdown or FZD4 overexpression reversed the effects of si-circ_0049271 on the H/R-induced H9c2 cells; that is, miR-17-3p knockdown or FZD4 overexpression promoted H/R-induced injury in the H9c2 cells.

Conclusions: Circ_0049271 promoted cellular function damage (e.g., proliferation inhibition, apoptosis, oxidative stress, and inflammation) in H/R-induced H9c2 cardiomyocytes via the miR-17-3p/FZD4 signaling axis.

Keywords: Acute myocardial infarction (AMI); cardiomyocyte injury; circ_0049271; miR-17-3p; FZD4

Page 2 of 16

Liao et al. Study of circ_0049271 in H/R-induced cardiomyocyte injury

Introduction

Acute myocardial infarction (AMI) is a heart-related disease with high morbidity and mortality, and the most serious cardiovascular disease in the world. In recent years, the incidence of AMI has increased year-by-year and has shown an increasing trend in younger individuals (1). With >790,000 AMI cases reported annually in the United States alone, AMI has become a prominent public health and social problem (1).

AMI is mainly caused by coronary occlusion, which not only results in the ischemic necrosis of cardiac tissue but also causes significant and irreversible damage to myocardial cells. The most prominent feature of AMI is myocardial damage caused by acute or persistent ischemia and hypoxia (2). Current clinical treatments for AMI include surgical interventions, interventional therapy, and thrombolysis. However, researchers have noted that these treatments can cause additional reperfusion injuries, such as myocardial cell death and microvascular system damage (3). There is accumulating evidence that myocardial infarction (MI) can lead to cardiac remodeling and further damage the heart (4). Inflammation and myocardial fibrosis are also key biological processes in cardiac remodeling after AMI (4). The inhibition of the cardiac inflammatory response has been shown to suppress infarction-induced cardiomyocyte apoptosis and inhibit myocardial fibrosis-mediated ventricular remodeling (5). Due to the insufficient regenerative capacity of the body's cardiomyocytes, it is important to develop effective alternatives to treat AMI and reduce cardiomyocyte loss.

Circular ribonucleic acid (circRNA) is an endogenous non-coding RNA characterized by a covalently closed cyclic structure. Due to its specific structure, circRNA has good stability, a long duration of action, and good resistance to RNA exonuclease (6). Additionally, circRNAs can adsorb micro RNAs (miRNAs) to regulate the expression of miRNAs and their downstream target genes. Through the above process, circRNAs perform extensive biological functions in various diseases, such as osteoporosis (7), cardiovascular diseases (8), nervous system diseases (9,10), and cancer (11). Thus, circRNAs have become a research hot spot in recent years, leading researchers to pay more attention to the important role of circRNAs in the pathophysiology of cardiovascular diseases. For example, Zhou *et al.* reported that circRNA ACR (Autophagy related cyclic) targets Pink1-mediated FAM65B phosphorylation to inhibit the autophagy and death of cardiomyocytes, thereby alleviating cardiomyocyte injury (12). Li *et al.* found that the knockdown of circRNA circ-BNIP3 reversed the effects of hypoxia on the viability and apoptosis on the H9c2 cells via the miR-27a-3p/BNIP3 pathway (13).

The above findings suggest that circRNAs might be the key targets of AMI-mediated cardiomyocyte injury. However, the current literature on AMI-related circRNAs is not comprehensive. In addition, circRNAs mainly function by adsorbing microRNAs. As endogenous small non-coding RNAs with a length of 19–25 nt, miRNAs can bind to the 3'-untranslated region of target genes to play a role in degrading messenger RNA (mRNA) and blocking mRNA translation (14). Several studies have shown that miRNAs are related to various diseases and injuries, including AMI (15) and spinal cord injury (16). For example, Yuan *et al.* discovered that an increase in miR-21 level significantly reduced the MI area caused by AMI and inhibited cardiomyocyte apoptosis (17). MiR-17-3p was shown to target Par4 (Protease activated receptor 4) to regulate cell survival, growth, apoptosis, and EMT (Epithelial mesenchymal transition) and inhibit mouse cardiac fibroblast senescence (18). MiRNAs also play an important role in the progression of AMI.

In this study, we first conducted a differential analysis to screen the highly expressed circRNAs in AMI, and total 6 potential circRNAs (hsa_circ_0037516, chr16:15794592-15794782+, chr3:16336362-1634509, hsa_circ_0049271, hsa_circ_0076767, and hsa_circ_0023461) were screened from GSE160717 and GSE169594 datasets. Ren et al found that circ_0023461 knockdown attenuated hypoxia-induced dysfunction in AC16 cells partly by targeting the miR-370-3p/PDE4D axis (19). There are no studies about the effect

---

Highlight box

Key findings
- Circ_0049271 promoted cellular function damage in hypoxia-reoxygenation–induced H9c2 cardiomyocytes via the miR-17-3p/FZD4 signaling axis.

What is known and what is new?
- The current literature on AMI-related circRNAs is not comprehensive. In addition, circRNAs mainly function by adsorbing microRNAs.
- We first conducted a differential analysis to screen the highly expressed circRNAs in AMI and identified circ_0049271, which was then used to further explore the cardiomyocyte function and mechanism.

What is the implication, and what should change now?
- Circ_0049271 may serve as a potential therapeutic target for AMI.

of chr16:15794592-15794782+, chr3:16336362-1634509 and hsa_circ_0076767 on AMI. The bioinformatics analyses have found that circ_0049271 is abnormally expressed and plays a biological role in lung cancer (20,21) and systemic lupus erythematosus (22). Meanwhile, circ_0049271 might be related to diabetic foot ulcer infectious inflammation (23). We speculate that circ_0049271 may play a role in inflammation in myocardial injury, so we chose circ_0049271 for further exploring the cardiomyocyte function and mechanism. Using Cell Counting Kit-8 (CCK-8) and apoptosis assays, the effects of circ_0049271 on the proliferation and apoptosis of AMI cells were evaluated. Further, the miRNAs and miRNA target genes interacting with circ_0049271 in the AMI and the molecular mechanism of action were also explored. We present the following article in accordance with the MDAR reporting checklist (available at https://atm.amegroups.com/article/view/10.21037/atm-22-6331/rc).

Methods

Clinical sample collection

Blood samples were collected from AMI patients diagnosed and treated at Huizhou Third People's Hospital from November 2021 to February 2022 and healthy (normal) volunteers during the same period. The study was conducted in accordance with the Declaration of Helsinki (as revised in 2013). All the research procedures were approved by the Research Ethics Committee of Huizhou Third People's Hospital (No. 2022-8). The blood samples were collected after the participants voluntarily signed the informed consent. Peripheral blood mononuclear cells (PBMCs) were immediately isolated from the blood samples using Ficoll density gradient centrifugation.

To be eligible for inclusion in this study, the patients had to meet the following inclusion criteria: (I) meet the World Health Organization's diagnostic criteria for AMI; (II) have a clinical and imaging diagnosis of AMI; and (III) have signs or clinical symptoms of AMI. Patients were excluded from the study if they met any of the following exclusion criteria: (I) had an onset time >24 h; (II) had severe liver and kidney failure, a malignant tumor, a primary disease of the nervous system, or a mental illness; and/or (III) were a lactating or pregnant female.

Cell culture and transfection

Rat cardiomyocytes H9c2, purchased from the National Collection of Authenticated Cell Cultures (Shanghai, China), were cultured in Dulbecco's modified eagle medium with 10% fetal bovine serum (FBS, Gibco, USA) and 1% penicillin-streptomycin (Gibco, USA). The medium was placed in an incubator at 37 ℃ with 5% carbon dioxide. The cells were divided into the normal group and the hypoxia-reoxygenation (H/R) group. In the normal group, the H9c2 cells were cultured normally. Then we established the H/R-induced H9c2 cell model according to a previous study (24). Briefly, the H9c2 cells were maintained in serum-free DMEM (dulbecco's modified eagle medium) without glucose and cultured in a hypoxic incubator which contained 1% O_2, 5% CO_2 and 94% N_2 for 24 h. Then the cells were reoxygenated (95% air/5% CO_2) in fresh DMEM with 10% FBS for 2 h.

GenePharma (China) designed and synthesized the circ_0049271 interference fragment (si-circ_0049271) and its control (si-NC, negative control siRNA), circ_0049271 overexpression plasmid (circ_0049271), and its no-load control (Vector), the miR-17-3p mimic and its control (NC mimic), and the miR-17-3p inhibition agent (miR-17-3p inhibitor) and its control (NC inhibitor). After culturing to a logarithmic growth phase, the H9c2 cells were digested, collected and diluted to 2×10^6 cells/mL. Subsequently, the cells were seeded in 6-well plates. When cell confluence reached about 70%, the above small RNAs or plasmids were transfected into the cells using Lipofectamine 2000 (Invitrogen, USA). After 48 h of culture, the cells were collected.

Bioinformatics analysis

AMI-related circRNA expression datasets (GSE169594 and GSE160717) were obtained from the Gene Expression Omnibus (GEO) database (https://www.ncbi.nlm.nih.gov/geo/) (Table 1). We performed a differential analysis of the circRNA expression data in the AMI and corresponding control samples in the GSE data sets using limma package. A (log fold change) >1 was used as the cut-off criterion to define DE-circRNAs. The intersection of the upregulated DE-circRNAs from the GSE169594 data set (191 DE-circRNAs) and GSE160717 data set (201 DE-circRNAs) was then analyzed and screened by Venny 2.1.0 (https://bioinfogp.cnb.csic.es/tools/venny/) (25).

Quantitative reverse transcription-polymerase chain reaction (qRT-PCR)

The cell nucleus RNA and cytoplasm RNA were separated

Page 4 of 16

Liao et al. Study of circ_0049271 in H/R-induced cardiomyocyte injury

Table 1 The basic information of the GEO data sets (GSE169594 and GSE160717)

GEO accession	Samples	Experiment type	Platforms
GSE169594	MCS, 4. AMI, 4.	Non-coding RNA profiling by array	GPL21825
GSE160717	NC, 3. AMI, 3.	Non-coding RNA profiling by array	GPL21825

GEO, Gene Expression Omnibus; MCS, mild coronary stenosis; AMI, acute myocardial infarction; NC, normal control.

Table 2 qRT-PCR primers

RNA	Sequences (5' to 3')
Circ_0049271	F: AACTTCGCTGAGCAGATTGG
	R: GCATGGGGTTCCAGAAGATA
Mir-17-3p	F: GCTCTGAUGUUCACGGAAGUG
	R: GTGCAGGGTCCGAGGT
FZD4	F: TTCACACCGCTCATCCAGTACG
	R: ACGGGTTCACAGCGTCTCTTGA
GAPDH	F: GTCTCCTCTGACTTCAACAGCG
	R: ACCACCCTGTTGCTGTAGCCAA
U6	F: CTCGCTTCGGCAGCACAT
	R: TTTGCGTGTCATCCTTGCG

qRT-PCR, quantitative reverse transcription-polymerase chain reaction.

in accordance with the instructions of the Cytoplasmic and Nuclear RNA Purification Kit (Cat. 21000, Norgen Biotek, Canada). Briefly, the cells were lysed using Lysis Buffer J and then centrifuged to separate cell fractions (pellet: nuclear fraction; supernatant: cytoplasmic fraction).

The supernatant and pellet were mixed with Buffer SK and absolute ethyl alcohol, respectively. Then combined the two mixtures with the centrifuge columns. Washed the columns with Wash Solution A. Finally, eluted the nuclear RNA and cytoplasmic RNA from centrifuge columns using Elution Buffer E.

The Trizol reagent was used to extract the total RNA from the cells and PBMCs of the peripheral blood. The concentration and purity of the RNA were then detected using NanoDrop. Subsequently, complementary deoxyribonucleic acid was prepared in accordance with the PrimeScript RT kit's instructions (Takara, Japan). Finally,

the expression levels of circ_0049271, miR-17-3p, and FZD4 were determined according to the fluorescence polymerase chain reaction (PCR) kit's instructions (Takara, Japan). U6 or glyceraldehyde-3-phosphate dehydrogenase (GAPDH) was used as the internal control, and the experiment was replicated 6 time. For the experimental data obtained by qRT-PCR, the $2^{-\Delta\Delta Ct}$ method was used to calculate the relative expression level of target gene. The sequences of the primer used for this step are shown in *Table 2*.

CCK-8

A CCK-8 kit (Beyotime, China) was used to measure the cell proliferation rate. Specifically, in accordance with the instructions of the CCK-8 kit, the cells were digested, collected, and seeded in a 96-well plate at 1×10^4 cells/well. After the cells adhered to the wall, different treatments were performed. After 0 and 24 h of treatment, the cells were assayed following the instructions of the CCK-8 kit. Then, 20 µL of CCK-8 reagent and the cells were incubated at 37 ℃ for 2–4 h, and the optical density (OD) was measured at 450 nm using an enzyme-labeled-instrument to calculate the cell proliferation rate. Additionally, 6 duplicate wells were set up in the experiment, and the experiment was repeated 3 times.

Flow cytometry

After being digested by trypsin, the H9c2 cells were collected in centrifuge tubes. Next, the cells were rinsed twice with pre-cooled sterile phosphate-buffered saline (PBS). Subsequently, the cell concentration was adjusted to 5×10^5 cells/mL, and the apoptosis was measured in accordance with the instructions of the Annexin V—Fluorescein Isothiocyanate (FITC) Apoptosis Detection Kit (Beyotime, China). Finally, apoptotic cells marked with positive FITC and positive/negative PI were detected by flow cytometry.

Biochemical tests

The culture supernatant of the cells was collected after centrifugation at 2,000 r/min for 10 min at 4 ℃. Next, the cells were digested with trypsin and collected into centrifuge tubes. The cells were then washed twice with pre-cooled sterile PBS to obtain the cell suspension, and then underwent homogenization. Subsequently, the cell

slurry was collected by centrifugation. Finally, the activities of creatine kinase (CK) and lactate dehydrogenase (LDH) in the culture supernatant and the level of malondialdehyde (MDA), reactive oxygen species (ROS), and superoxide dismutase (SOD) in the cells were detected in accordance with the instructions of the corresponding biochemical kit (Jiancheng, Nanjing).

Enzyme-linked immunosorbent assays (ELISAs)

The cell suspension was collected. The contents of IL-1β, IL-6, and IL-8 in the suspension were determined in accordance with the instructions of the ELISA kit (Shanghai Enzyme-linked Biotechnology Co., Ltd., China). Finally, microplate readers were used to measure the OD at 450 nm (OD450).

Western blot

Radio immunoprecipitation assay lysis buffer (RIPA) cell lysate (Solebo, China) was used to extract the total protein of the cells, and the concentration of the extracted protein was determined using a bicinchoninic acid kit. Next, 20 μg of the proteins were separated by sodium dodecyl sulfate-polyacrylamide gel electrophoresis. The proteins were then transferred onto polyvinylidene fluoride membranes, blocked in 5% non-fat dry milk for 1–3 h, and primary antibodies [Bax, Bcl-2 (B-cell lymphoma-2), c-caspase-3, and GAPDH, Cell Signal Tech, USA] were added for incubation overnight at 4 ℃. Subsequently, the membranes were washed 3 times with tris-buffered saline and incubated in the secondary antibody dilution buffer for 1 h at ambient temperature. After washing the membranes 3 more times, enhanced chemiluminescence reagent (Solebo, China) was dripped onto the membranes. Subsequently, the membranes were placed in a gel imaging system to conduct protein development and image collection. ImageJ software was used to analyze the gray level of the protein bands, and GAPDH was used as the internal control to calculate the relative protein expression.

Dual-luciferase reporter gene

CircMIR 1.0 software and Targetscan 7.0 (http://www.targetscan.org/vert_70/) were used to predict the binding sites of circ_000049271 and miR-17-3p and miR-17-3p and FZD4, respectively. The wild-type (WT) or mutant (MUT) fragment of circ_0049271 or FZD4 was constructed into the dual-luciferase reporter plasmids (GP-miRGLO) (GenePharma). After the confluence reached about 80%, the 293T cells were co-transfected with the luciferase reporter plasmids and miR-17-3p mimic or NC mimic. The luciferase activity was measured using a dual-luciferase reporter kit 48 h after transfection (Promega, USA).

RNA pull-down

Biotinylated miR-17-3p (miR-17-3p-bio) and biotinylated control miR-NC (miR-NC-bio) were constructed. Specifically, the cell extracts (2 μg) were incubated with biotinylated RNA (100 pmol) for 1 h, and agarose beads (Invitrogen) were added for another 1 h of incubation. RNA was extracted, and the expression level of FZD4 or circ_0049271 in the precipitated complex was further detected using qRT-PCR.

Statistical analysis

All the results are expressed as the mean ± standard deviation (SD). The SPSS v26.0 software was used to perform the 1-way analyses of variance for comparisons among multiple groups and the t-test analyses for comparisons between 2 groups. Pearson correlation was used to analyze the correlations of the expression of circ_0049271, miR-17-3p, and FZD4 in the clinical blood samples. A P value <0.05 was used as the criterion for determining significant statistical difference.

Results

Circ_0049271 was significantly upregulated in the blood and H/R-induced H9c2 cells of the AMI patients

A differential analysis was performed on the AMI-related circRNA expression GEO data sets of GSE169594 and GSE160717. Next, 191 and 201 DE-circRNAs were screened from the GSE169594 and GSE160717 data sets (see Tables S1,S2). The intersections of the significantly upregulated circRNAs in the GSE169594 and GSE160717 data sets were analyzed using a Venn diagram (*Figure 1A*). The results of the intersections identified 6 potential circRNAs (i.e., hsa_circ_0037516, chr16:15794592-15794782+, chr3:16336362-1634509, hsa_circ_0049271, hsa_circ_0076767, and hsa_circ_0023461), from which, circ_0049271 was selected for the further cell experiments.
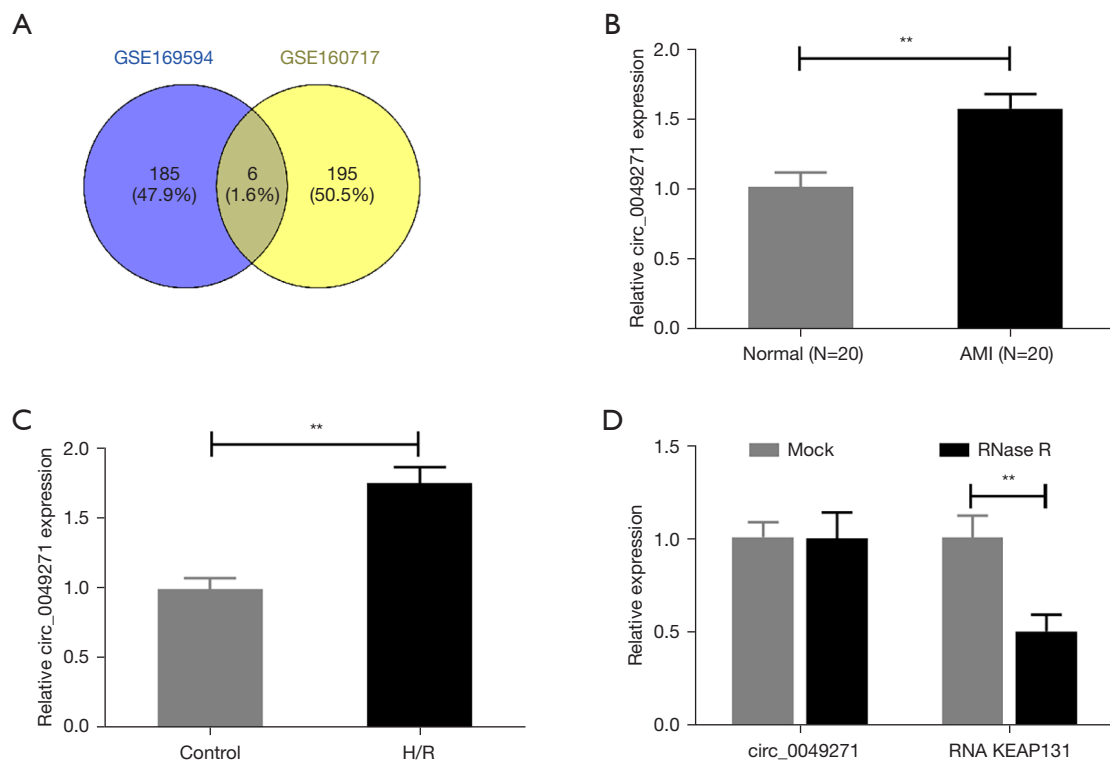
Figure 1 Circ_0049271 was significantly upregulated in the blood and hypoxia-induced H9c2 cells of the AMI patients. (A) A Venn diagram showed the significant upregulation of differential circRNA expression in both the GSE169594 and GSE160717 data sets; (B,C) qRT-PCR was used to detect the circ_0049271 expression in the AMI clinical samples (B) and hypoxia-induced H9c2 cells (C); (D) qRT-PCR was used to determine the circ_0049271 expression level after RNase R treatment, **, $P<0.01$. H/R, hypoxia-reoxygenation; RNase R, Ribonuclease R; AMI, acute myocardial infarction; qRT-PCR, quantitative reverse transcription-polymerase chain reaction.

Next, qRT-PCR was used to detect circ_0049271 expression in the AMI clinical blood samples and hypoxia-induced H9c2 cells. As a result, the circ_0049271 expression levels in the blood sample of the patients in the AMI group and H9c2 cells in the H/R group were significantly higher than those in the corresponding Normal group and Control group (*Figure 1B,1C*, $P<0.01$). In addition, the circ_0049271 maintained a stable closed-loop structure after RNase R (Ribonuclease R) treatment (*Figure 1D*), which suggests that circ_0049271 is significantly highly expressed in AMI.

Effects of Circ_0049271 on the proliferation and apoptosis of the H/R-induced H9c2 cells

Circ_0049271 knockdown or overexpression was performed in the H/R-induced myocardial H9c2 cells to explore the function of circ_0049271 in H/R-induced myocardial H9c2 cell injury (*Figure 2A*). Cell proliferation was detected by CCK-8, and apoptosis was detected by flow cytometry

and Western Blot. The CCK-8 results showed that the si-circ_0049271 group exhibited a significantly increased proliferation level in the H9c2 cells compared to the si-NC group. However, the proliferation level of cells in the circ_0049271 group was significantly lower than that in the Vector group (*Figure 2B*, $P<0.05$). Additionally, the flow cytometry results indicated that circ_0049271 knockdown significantly reduced the apoptosis rate of the cells ($P<0.05$). However, the overexpression of circ_0049271 significantly increased cell apoptosis ($P<0.01$) (*Figure 2C,2D*). The Western blot results showed that the expression level of the pro-apoptotic proteins (i.e., Bax and c-caspase-3) was significantly decreased, and the expression level of the anti-apoptotic Bcl-2 in the cells after si-circ_0049271 knockdown was significantly increased. After circ_004927 overexpression, the protein expression of Bax, c-caspase-3, and Bcl-2 showed the opposite results to those produced by the si-circ_0049271 knockdown (*Figure 2E*). These outcomes suggested that the knockdown of circ_0049271
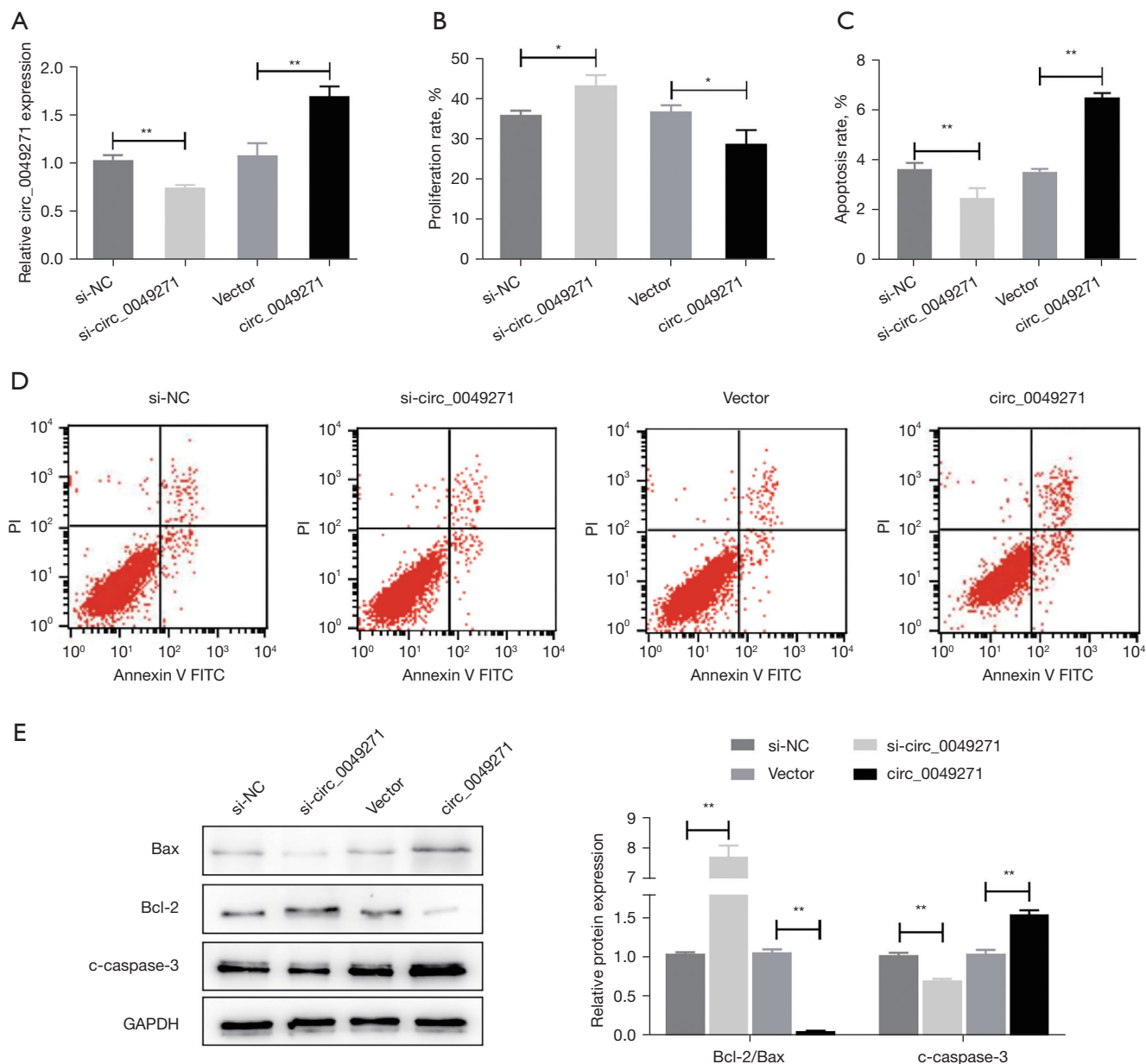
Figure 2 Effects of circ_0049271 on the proliferation and apoptosis of the H9c2 cells with H/R-induced myocardial injury. (A) qRT-PCR was used to detect the circ_0049271 expression level in the cells after the knockdown or overexpression of circ_0049271; (B) CCK-8 was used to detect cell proliferation; (C,D) Flow cytometry was used to detect cell apoptosis; (E) Western blot was used to detect the protein expression of Bax, c-caspase-3, and Bcl-2. *, $P<0.05$, **, $P<0.01$. si-NC group, H9c2 cells transfected with the negative control of siRNA. si-circ_0049271 group, H9c2 cells transfected with the circ_0049271 siRNA. Vector group, H9c2 cells transfected with the negative control plasmid. circ_0049271 group, H9c2 cells transfected with the circ_0049271 overexpression plasmid. si-NC, negative control siRNA; PI, isoelectric point; FITC, Fluorescein Isothiocyanate; H/R, hypoxia-reoxygenation; qRT-PCR, quantitative reverse transcription-polymerase chain reaction; CCK-8, Cell Counting Kit-8.

promoted proliferation and inhibited apoptosis in the H/R-induced myocardial injury cells (i.e., the H9c2 cells).

Effects of circ_0049271 on the damage, oxidative stress, and inflammatory response of the H/R-induced H9c2 cells

It was previously reported that the level of myocardial enzymes (CK and LDH) were abnormally increased during myocardial hypoxia-ischemia (26). In this study, we measured the level of related substances to assess whether circ_0049271 could improve H/R-induced injury, oxidative stress, and inflammatory responses in the H9c2 cells. The level of myocardial enzymes (CK and LDH), oxidative stress substances (ROS, MDA, and SOD) and inflammatory factors (IL-1β, IL-6, and IL-8) were determined. The results revealed that after the knockdown of circ_0049271, the activities of LDH and CK and the level of ROS, MDA, IL-1β, IL-6, and IL-8 in the H/R-induced H9c2 cells were significantly decreased, while SOD activity was significantly increased. However, the opposite trend was observed when circ_0049271 was overexpressed in the H/R-induced H9c2 cells; that is, the activities of LDH and CK and the level of ROS, MDA, IL-1β, IL-6, and IL-8 were significantly increased, while SOD activity was significantly decreased (*Figure 3A-3H*, P<0.05). Thus, the knockdown of circ_0049271 was shown to significantly alleviate the damage, oxidative stress, and inflammatory response of the H/R-induced H9c2 cells.

Circ_0049271 serves as a sponge for MiR-17-3p

To explore the mechanism of action of circ_0049271, we localized circ_0049271 and found that it was mainly distributed in the cytoplasm (*Figure 4A*). Further, the results of the circbank (http://www.circbank.cn/searchCirc.html) database revealed a relationship between circ_0049271 and miR-17-3p. The luciferase reporter gene experiments confirmed that the co-transfection of the miR-17-3p mimic significantly reduced the luciferase activity of the circ_0049271-WT vector but did not affect the luciferase activity of the circ_0049271-MUT vector (*Figure 4B*). Additionally, the RNA pull-down experiments confirmed the targeting relationship between circ_0049271 and miR-17-3p (*Figure 4C*). Further, in contrast to circ_0049271, the miR-17-3p expression level in the cells of the H/R group was much lower than that in the Control group (*Figure 4D*). The miR-17-3p expression level was significantly increased when circ_0049271 was decreased in the H9c2 cells, while

the miR-17-3p level was significantly decreased after circ_0049271 overexpression (*Figure 4E*). Additionally, circ_0049271 was negatively correlated with miR-17-3p expression in the AMI clinical blood samples (*Figure 4F*). Thus, circ_0049271 served as a sponge for miR-17-3p in the cytoplasm of the AMI cells, and miR-17-3p was lowly expressed in AMI.

FZD4 acts as a target of MiR-17-3p

The targeting relationship between miR-17-3p and FZD4 was predicted by the TargetScan database (https://www.targetscan.org/vert_80/) and further examined by dual-luciferase reporter and RNA pull-down experiments (*Figure 5A-5C*). The qRT-PCR results showed that the expression level of FZD4 was significantly higher in the cells of the H/R group than the Control group (*Figure 5D*). Additionally, miR-17-3p in the cells was knocked down or overexpressed by transfection (*Figure 5E*). The transfection results revealed a negative association between the mRNA and protein expression levels of FZD4 and the miR-17-3p level in the cells (*Figure 5F-5H*). FZD4 was also negatively correlated with miR-17-3p in the AMI clinical blood samples (*Figure 5I*). In addition, the FZD4 expression level in the cells was significantly reduced after the knockdown of circ_0049271, while the overexpression of circ_0049271 markedly upregulated the expression level of FZD4 (*Figure 5J*). According to the Pearson correlation analysis, circ_0049271 was positively correlated with FZD4 expression level in the AMI clinical blood samples (*Figure 5K*). These results suggested that FZD4 not only acted as the target gene of miR-17-3p but was also highly expressed in AMI. Further, FZD4 may also function as an oncogene in AMI.

MiR-17-3p knockdown or FZD4 overexpression reverses the effects of si-circ_0049271 on the H/R-induced H9c2 cells

To verify whether circ_0049271 plays a role in AMI through miR-17-3p/FZD4, the H/R-induced H9c2 cells were treated as follows. Circ_0049271 and miR-17-3p were simultaneously knocked down (si-circ_0049271 + miR-17-3p inhibitor group), while circ_0049271 was knocked down, and FZD4 was upregulated (si-circ_0049271 + FZD4 group). The treatment results showed that after the knockdown of circ_0049271, the FZD4 protein expression level was increased by further inhibiting the miR-17-3p
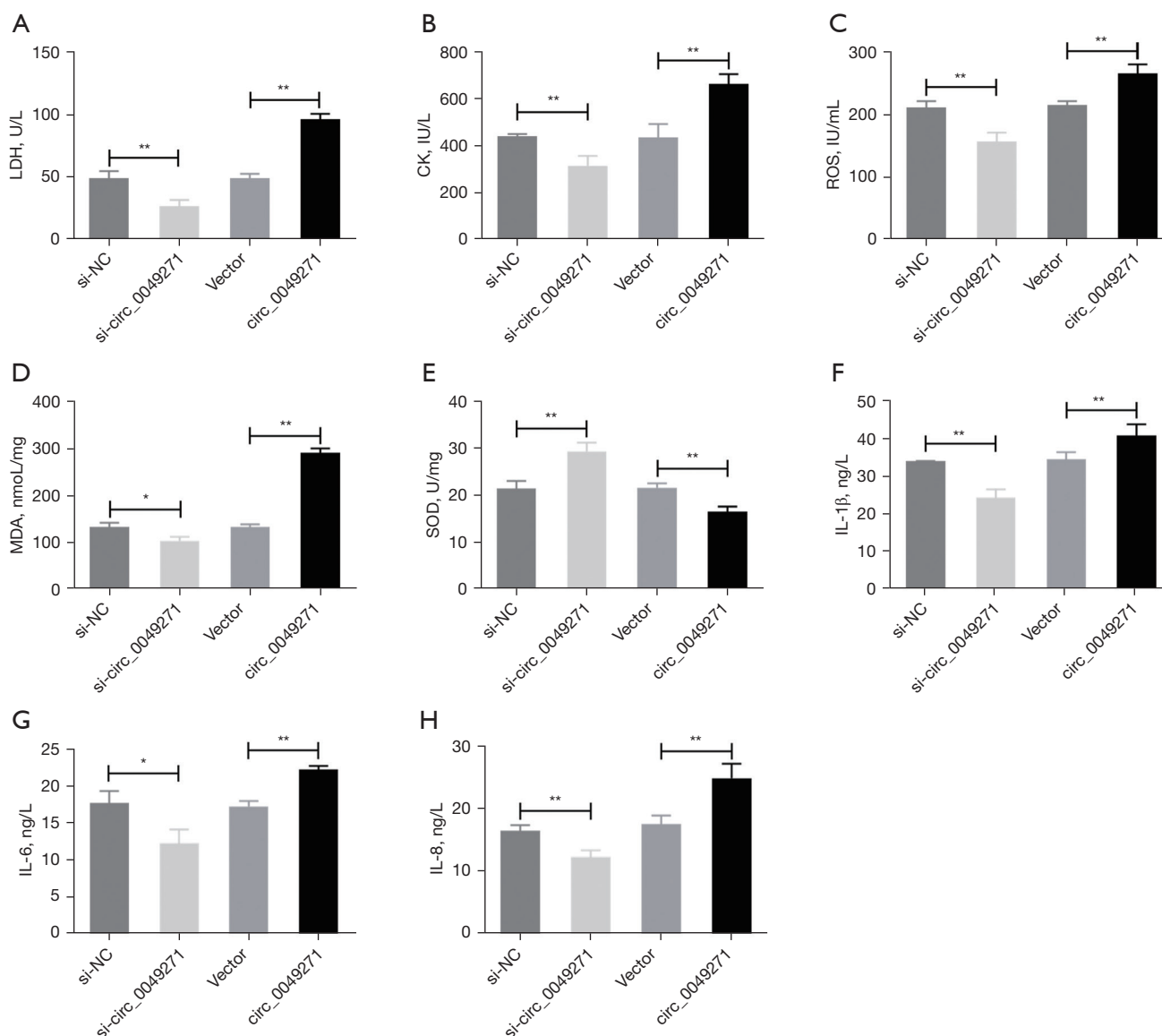
Figure 3 Effects of circ_0049271 on injury, oxidative stress, and inflammatory response in the H/R-induced H9c2 cells. (A-E) A biochemical test was used to determine the level of the myocardial enzymes [LDH (A) and CK (B)] and oxidative stress substances [ROS (C), MDA (D), SOD (E)] in the H/R-induced H9c2 cells after the knockdown or overexpression of circ_0049271; (F-H) ELISA was used to detect the level of inflammatory factors (IL-1β, IL-6, and IL-8) in the H/R-induced H9c2 cells after the knockdown or overexpression of circ_0049271. **, $P<0.01$; *, $P<0.05$. LDH, lactate dehydrogenase; si-NC, negative control siRNA; CK, creatine kinase; ROS, reactive oxygen species; MDA, malondialdehyde; SOD, superoxide dismutase; IL, interleukin; H/R, hypoxia-reoxygenation; ELISA, enzyme-linked immunosorbent assay.

expression or overexpression of FZD4 in the H/R-induced H9c2 cells (*Figure 6A,6B*). In sequence, the proliferation, apoptosis, injury, oxidative stress, and inflammatory response of the cells in each group were detected, and the results indicated that the further inhibition of miR-17-3p expression or the overexpression of FZD4 significantly reduced the cell proliferation rate (*Figure 6C*). Additionally, the further inhibition of miR-17-3p expression or the overexpression of FZD4 increased the cell apoptosis rate, promoted the expression of pro-apoptotic-related proteins (c-caspase-3 and Bax), and inhibited the expression of anti-apoptosis-related protein Bcl-2 (*Figure 6D-6G*). Further,

Page 10 of 16

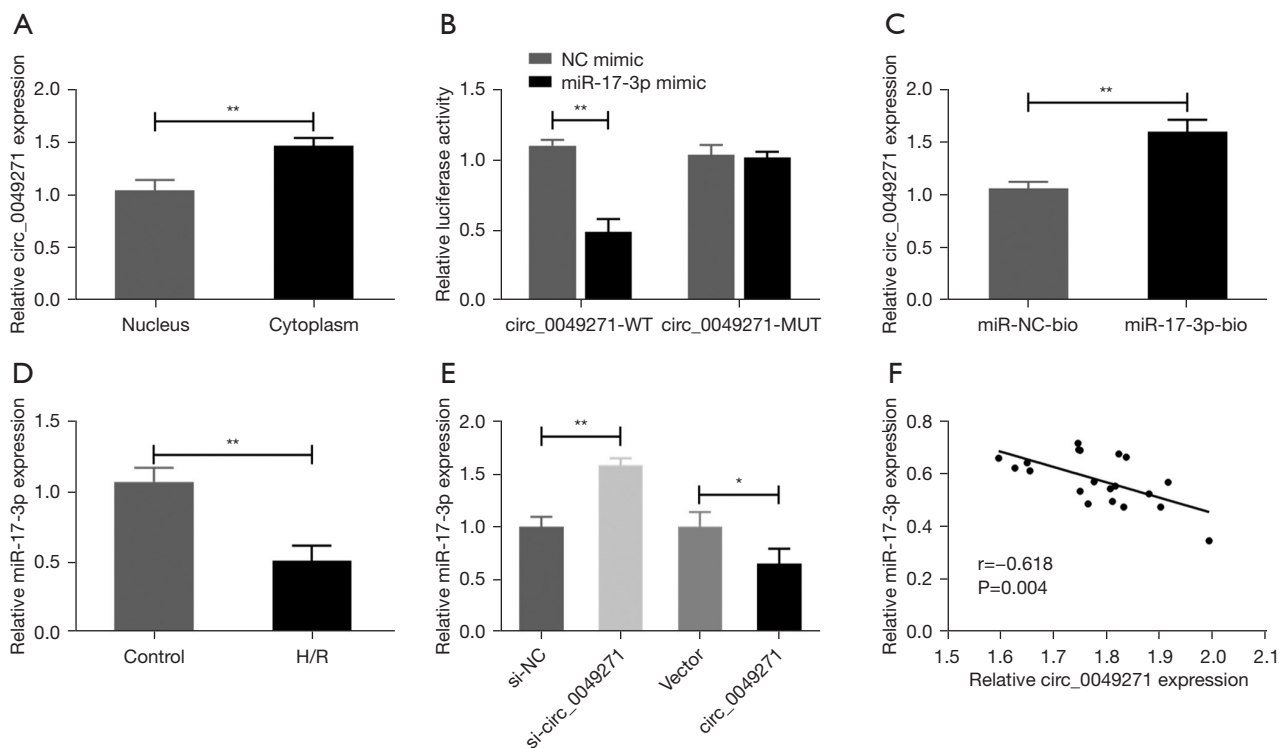Liao et al. Study of circ_0049271 in H/R-induced cardiomyocyte injury

Figure 4 Circ_0049271 served as a sponge for miR-17-3p. (A) qRT-PCR showing circ_0049271 expression levels in the cytoplasm and nucleus. (B) Dual luciferase experiments were used to verify the targeting relationship between circ_0049271 and miR-17-3p, **, $P<0.01$ *vs.* miR-17-3p group; (C) RNA pull-down experiments were used to verify the targeting relationship between circ_0049271 and miR-17-3p; (D,E) qRT-PCR was used to detect the miR-17-3p expression level in the H/R-induced H9c2 cells of H/R group (D) and the miR-17-3p expression levels in the H9c2 cells after the knockdown or overexpression of circ_0049271 (E); (F) a Pearson correlation analysis was performed to evaluate the correlation between circ_0049271 and miR-17-3p expression in the AMI clinical blood samples. **, $P<0.01$; *, $P<0.05$. NC, negative control; WT, wild-type; MUT, mutant; H/R, hypoxia-reoxygenation; si-NC, negative control siRNA; qRT-PCR, quantitative reverse transcription-polymerase chain reaction; AMI, acute myocardial infarction.

H/R-induced H9c2 cell damage, oxidative stress (ROS and MDA) and inflammatory responses were also promoted by some other different treatments, which included increasing the activity of the myocardial enzymes (CK and LDH), and regulating the secretion of the oxidative stress substances and inflammatory factors (*Figure 6H-6O*). To sum up, the knockdown of miR-17-3p or the overexpression of FZD4 reversed the pro-proliferation, anti-apoptosis, anti-oxidative stress, and anti-inflammatory effects of si-circ_0049271 on the H/R-induced H9c2 cells.

Discussion

With the advancement and popularization of high-throughput technology, researchers have discovered that circRNA is a non-coding circular endogenous RNA molecule produced by special alternative splicing (27). CircRNA plays a significant role in various human diseases, including cardiovascular disease (28). It has been reported that some circRNAs [e.g., circ_0060745 (29), circSAMD4A (30), circCDYL (31), and circ_LAS1L (32) affect myocardial cell injury in AMI. At present, the corresponding mechanisms of the above circRNAs have been explored. In our study, the significantly upregulated circRNAs in the AMI-related data sets GSE169594 and GSE160717 were intersected, and 6 common significantly upregulated circRNAs (i.e., hsa_circ_0037516, chr16: 15794592-15794782+, chr3: 16336362-1634509, hsa_circ_0049271, hsa_circ_0076767, and hsa_circ_0023461) were identified. Ren *et al.* found that circ_0023461 expression was upregulated in AMI patients and hypoxia-induced AC16 cells, and the knockdown of circ_0023461 targeted the miR-370-3p/PDE4D axis to
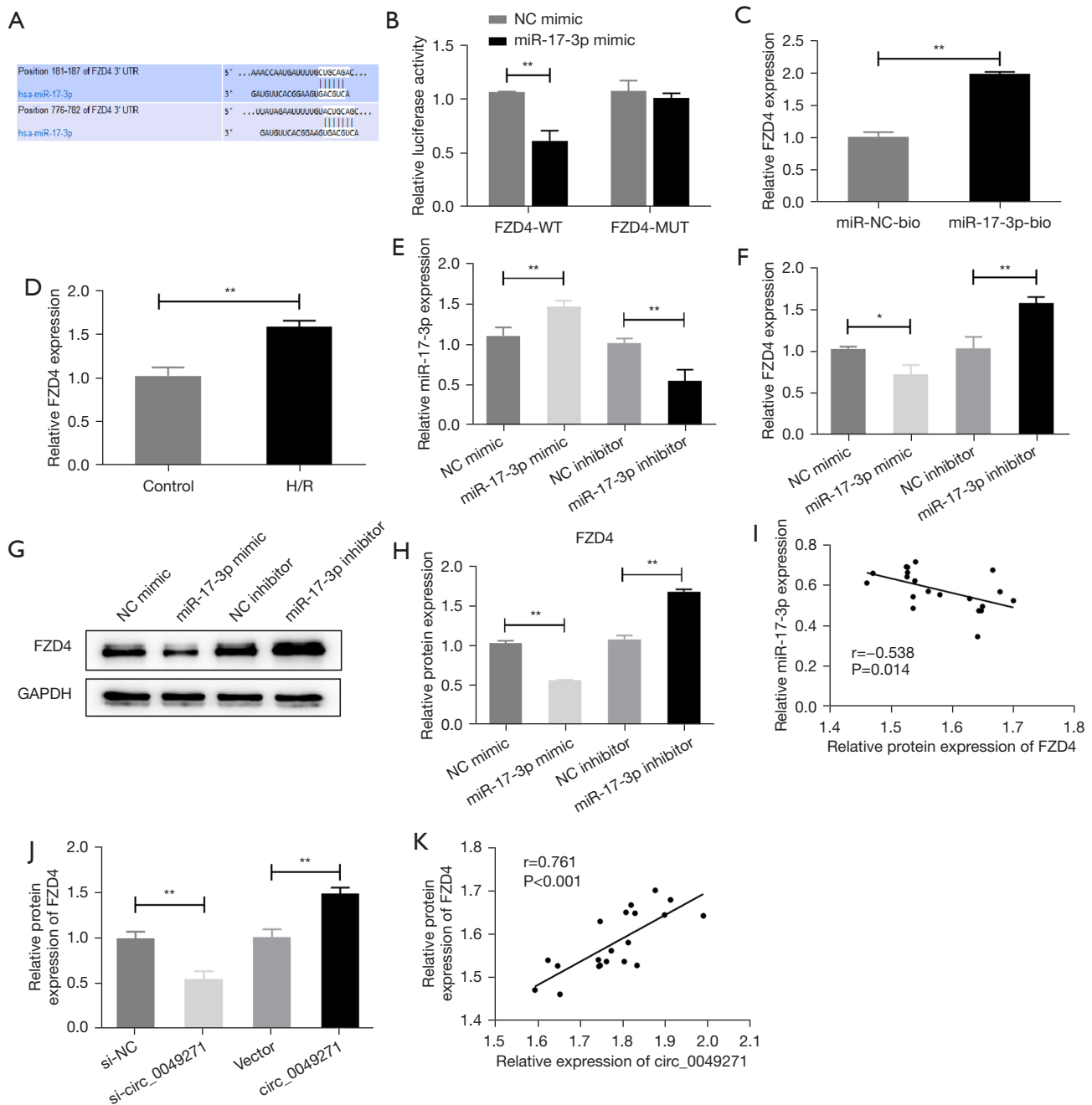
Figure 5 FZD4 acts as the target of miR-17-3p. (A) The targeting sites were predicted by the TargetScan Online website. (B) Dual-luciferase experiments were used to verify the targeting relationship between miR-17-3p and FZD4; (C) RNA pull-down experiments were used to confirm the targeting relationship between miR-17-3p and FZD4; (D-F) qRT-PCR was used to detect the mRNA expression level of FZD4 in the H/R group cells (D), verify the efficiency of the knockdown or overexpression of miR-17-3p in the cells (E), and measure the mRNA expression level of FZD4 after the knockdown or overexpression of miR-17-3p in the cells (F); (G,H) Western blot was used to detect the FZD4 protein expression level after the knockdown or overexpression of miR-17-3p in cells; (I) a Pearson correlation analysis was conducted to analyze the correlation between miR-17-3p and FZD4 expression in the AMI clinical blood samples; (J) qRT-PCR was used to determine the mRNA expression level of FZD4 after the knockdown or overexpression of circ_0049271 in the cells; (K) a Pearson correlation analysis was conducted to analyze the correlation between circ_0049271 and FZD4 expression in the AMI clinical blood samples. **, $P<0.01$; *, $P<0.05$. NC, negative control; WT, wild-type; MUT, mutant; si-NC, negative control siRNA; H/R, hypoxia-reoxygenation; qRT-PCR, quantitative reverse transcription-polymerase chain reaction; AMI, acute myocardial infarction.
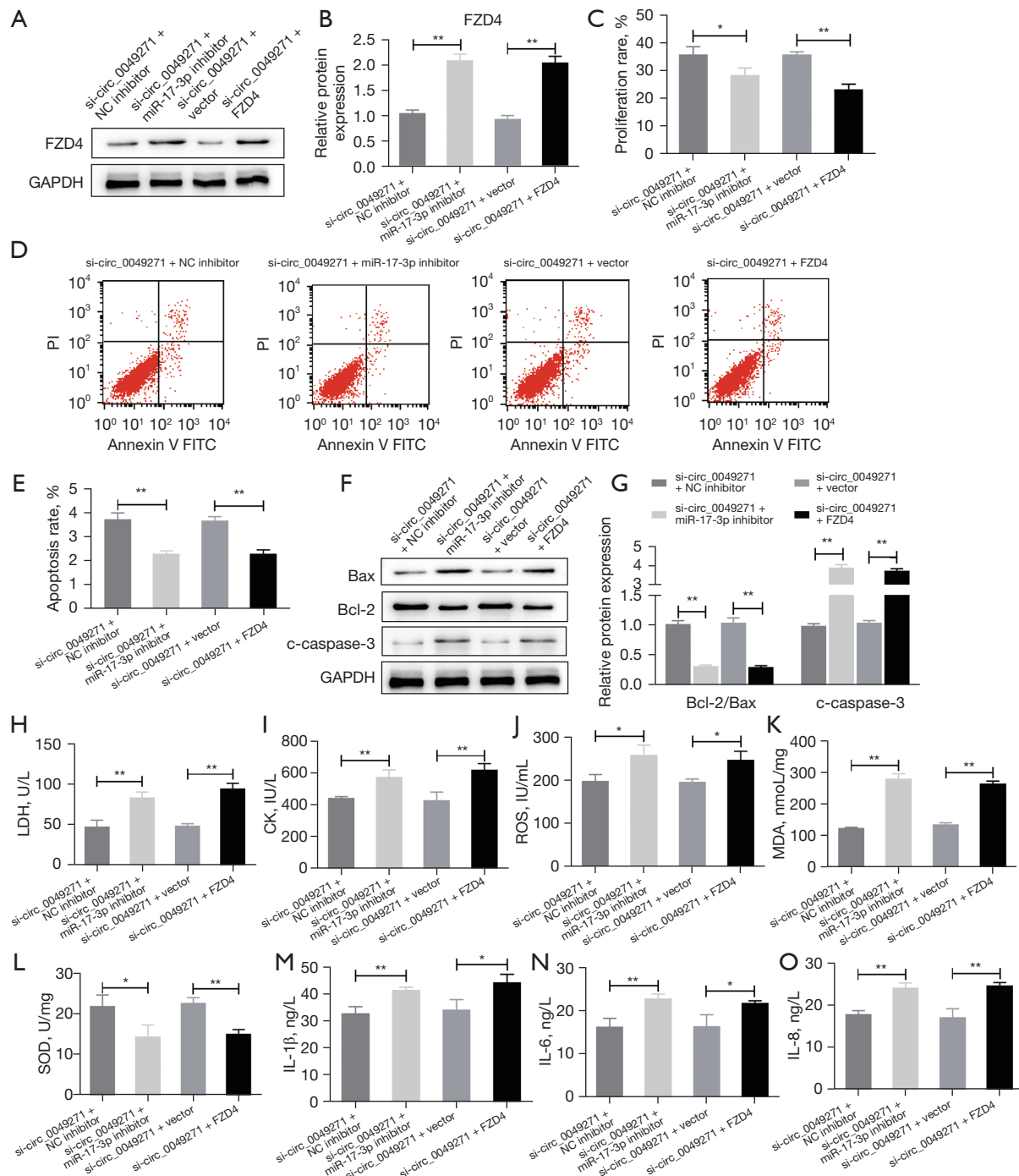
Page 12 of 16

Liao et al. Study of circ_0049271 in H/R-induced cardiomyocyte injury

Figure 6 MiR-17-3p knockdown or FZD4 overexpression reversed the effects of si-circ_0049271 on the H/R-induced H9c2 cells. (A,B) Western blot was used to detect the protein expression levels of FZD4 in each group of cells; (C) CCK-8 was used to measure the proliferation rate of each group of cells; (D,E) flow cytometry was used to determine the apoptosis rates of the cells; (F,G) Western blot was used to detect the protein expression levels of the apoptosis-related proteins (i.e., Bax, Bcl-2, and c-caspase-3) in the cells of each group; (H,I) biochemical tests were used to determine the activities of LDH and CK in each group of cells; (J-L) biochemical tests were used to determine the levels of the oxidative stress substances (i.e., ROS, MDA and SOD) in the cells of each group; (M-O) ELISA was used to detect the levels of the inflammatory factors (i.e., IL-1β, IL-6, and IL-8) in the cells of each group. **, $P<0.01$; *, $P<0.05$. NC, negative control; PI, isoelectric point; FITC, Fluorescein Isothiocyanate; LDH, lactate dehydrogenase; CK, creatine kinase; ROS, reactive oxygen species; MDA, malondialdehyde; SOD, superoxide dismutase; IL, interleukin; H/R, hypoxia-reoxygenation; ELISA, enzyme-linked immunosorbent assay.

alleviate hypoxia-induced AC16 cell dysfunction (19). However, to date, no studies have examined the functions of the other circRNAs in AMI. In this study, the role and mechanism of circ_0049271 in AMI were explored.

We found that circ_0049271 expression was significantly increased in the blood of the AMI patients and the H/R-induced H9c2 cells. Further, we found that circ_0049271 knockdown alleviated the proliferation inhibition and pro-apoptotic effects of the H/R-induced H9c2 cells, reducing the release of the oxidative stress substances and inflammatory factors, and improving cell damage. However, the overexpression of circ_0049271 produced the opposite effects to that of circ_0049271 knockdown. Given the crucial role of apoptosis and the injury of cardiomyocytes in AMI, it may be that circ_0049271 is involved in the pathogenesis of AMI.

As the target of circRNA, miRNA is the most widely studied non-coding RNA. Specifically, miRNA regulates cell proliferation, differentiation, and apoptosis by degrading target genes or inhibiting the translation (33). Further, miRNAs are involved in cardiac development, cardiac function regulation, cardiac remodeling, and cardiomyocyte apoptosis in the cardiovascular system (34). MiRNAs are also abnormally expressed in cardiovascular diseases (e.g., AMI, angina pectoris, and myocarditis) (35). A study has shown that miRNA-499, miRNA-1, miRNA-133, and miRNA-208 can serve as markers of myocardial injury in AMI (36). MiR-17-92 consists of 6 mature miRNAs (i.e., miR-17, miR-18a, miR-19a, miR-20a, miR-19b1, and miR-92a-1) and is one of the most widely studied miRNA clusters (29). Shi *et al.* showed that miR-17-3p promotes cardiomyocyte hypertrophy, proliferation, and survival and functional recovery after cardiac ischemia/reperfusion (37). Meanwhile, Yuan et al found that inhibition of miR-17-3p aggravated H/R-induced H9c2 injury, and promoted the expression of inflammatory mediators including tumor necrosis factor (TNF)-α, interleukin (IL)-6, IL-1β and phosphorylated NF-κB subunit p65 (38). The present study found that the expression level of miR-17-3p was significantly decreased in in the blood of the AMI patients and H/R-induced H9c2 cells. MiR-17-3p expression was also found to be negatively correlated with circ_0049271 expression. The targeting relationship between circ_0049271 and miR-17-3p was confirmed by dual-luciferase and RNA pull-down experiments. Based on the above outcomes in this study, we speculated that circ_0049271 might function through miR-17-3p.

FZD4, a member of the frizzled gene family, encodes the transmembrane receptor of the Wnt/β-catenin signaling protein (39). Studies have shown that FZD4 is not only abnormally expressed in various cancers (e.g., gastric cancer, breast cancer, non-small cell lung cancer, and liver cancer) but is also associated with the malignant behaviors of these cancers (40,41). In addition, FZD4 is also regulated by circRNA-miRNA. Notably, Zhou *et al.* found that the downregulation of circ_0004712 mediated the miR-331-3p/FZD4 pathway to inhibit the progression of ovarian cancer (42). Zhang *et al.* discovered that circ-ACAP2 promoted colorectal cancer progression by targeting the miR-143-3p/FZD4 axis (43). There are few studies on the function of FZD4 in cardiac injury. A study found that elevated Wnt2 and Wnt4 activate β-catenin/NF-κB signaling to promote cardiac fibrosis by cooperation of FZD4/2 and LRP6 in fibroblasts, which contributes to adverse outcome of patients with AMI (44). In our study, we observed that FZD4 expression was significantly upregulated in the blood of AMI patients and H/R-induced H9c2 cells. Further, FZD4 expression was found to be positively correlated with circ_0049271 and negatively correlated with miR-17-3p. In addition, the targeting relationship between miR-17-3p and FZD4 was further clarified by dual-luciferase and RNA pull-down experiments. FZD4 expression was observed to be significantly upregulated after circ_0049271 and miR-17 were knocked down simultaneously. The functional verification in this study showed that miR-17-3p knockdown or FZD4 overexpression reversed the effects of si-circ_0049271 on the proliferation, apoptosis, oxidative stress, and inflammation of the H/R-induced H9c2 cells. Thus, we conjecture that miR-17-3p/FZD4 is the key molecular mechanism for circ_0049271 affecting H/R-induced H9c2 cell injury.

The present study had some limitations. First, it only explored the function and mechanism of circ_0049271 in the induced AMI model cell-H9c2 cells and did not establish multiple AMI cell models for further verifications. Second, the AMI animal model was not established to verify the function and mechanism of circ_0049271. Thus, further experiments need to be conducted to examine the function and mechanism of circ_0049271.

Conclusions

The expression of circ_0049271 and FZD4 was upregulated

Page 14 of 16

Liao et al. Study of circ_0049271 in H/R-induced cardiomyocyte injury

while that of miR-17-3p was significantly downregulated in the blood of the AMI patients and H/R-induced H9c2 cells. In addition, the knockdown of circ_0049271 regulated the miR-17/FZD4 axis to promote cell proliferation, inhibit cell apoptosis and the secretion of oxidative stress substances and inflammatory factors, and improve the damage of the H/R-Induced H9c2 cells. Taken together, our results suggest that circ_0049271 could serve as a potential therapeutic target for AMI.

Acknowledgments

Footnote

References

1. Gulati R, Behfar A, Narula J, et al. Acute Myocardial Infarction in Young Individuals. Mayo Clin Proc 2020;95:136-56.

2. Shibata T, Kawakami S, Noguchi T, et al. Prevalence, Clinical Features, and Prognosis of Acute Myocardial Infarction Attributable to Coronary Artery Embolism. Circulation 2015;132:241-50.

3. Amsterdam EA, Wenger NK, Brindis RG, et al. 2014 AHA/ACC Guideline for the Management of Patients with Non-ST-Elevation Acute Coronary Syndromes: a report of the American College of Cardiology/American Heart Association Task Force on Practice Guidelines. J Am Coll Cardiol 2014;64:e139-e228.

4. Caballero EP, Santamaria MH, Corral RS. Endogenous osteopontin induces myocardial CCL5 and MMP-2 activation that contributes to inflammation and cardiac remodeling in a mouse model of chronic Chagas heart disease. Biochim Biophys Acta Mol Basis Dis 2018;1864:11-23.

5. Gan W, Ren J, Li T, et al. The SGK1 inhibitor EMD638683, prevents Angiotensin II-induced cardiac inflammation and fibrosis by blocking NLRP3 inflammasome activation. Biochim Biophys Acta Mol Basis Dis 2018;1864:1-10.

6. Panda AC. Circular RNAs Act as miRNA Sponges. Adv Exp Med Biol 2018;1087:67-79.

7. Yang Y, Yujiao W, Fang W, et al. The roles of miRNA, lncRNA and circRNA in the development of osteoporosis. Biol Res 2020;53:40.

8. Altesha MA, Ni T, Khan A, et al. Circular RNA in cardiovascular disease. J Cell Physiol 2019;234:5588-600.

9. Akhter R. Circular RNA and Alzheimer's Disease. Adv Exp Med Biol 2018;1087:239-43.

10. Zhang Z, Yang T, Xiao J. Circular RNAs: Promising Biomarkers for Human Diseases. EBioMedicine 2018;34:267-74.

11. Zhang HD, Jiang LH, Sun DW, et al. CircRNA: a novel type of biomarker for cancer. Breast Cancer 2018;25:1-7.

12. Zhou LY, Zhai M, Huang Y, et al. The circular RNA ACR attenuates myocardial ischemia/reperfusion injury by suppressing autophagy via modulation of the Pink1/FAM65B pathway. Cell Death Differ 2019;26:1299-315.

13. Li Y, Ren S, Xia J, et al. EIF4A3-Induced circ-BNIP3 Aggravated Hypoxia-Induced Injury of H9c2 Cells by Targeting miR-27a-3p/BNIP3. Mol Ther Nucleic Acids

2020;19:533-45.

14. Miao L, Yin RX, Zhang QH, et al. A novel circRNA-miRNA-mRNA network identifies circ-YOD1 as a biomarker for coronary artery disease. Sci Rep 2019;9:18314.

15. Xing X, Guo S, Zhang G, et al. miR-26a-5p protects against myocardial ischemia/reperfusion injury by regulating the PTEN/PI3K/AKT signaling pathway. Braz J Med Biol Res 2020;53:e9106.

16. Li B, Wang Z, Yu M, et al. miR-22-3p enhances the intrinsic regenerative abilities of primary sensory neurons via the CBL/p-EGFR/p-STAT3/GAP43/p-GAP43 axis. J Cell Physiol 2020;235:4605-17.

17. Yuan J, Chen H, Ge D, et al. Mir-21 Promotes Cardiac Fibrosis After Myocardial Infarction Via Targeting Smad7. Cell Physiol Biochem 2017;42:2207-19.

18. Lu D, Tang L, Zhuang Y, et al. miR-17-3P regulates the proliferation and survival of colon cancer cells by targeting Par4. Mol Med Rep 2018;17:618-23.

19. Ren K, Li B, Jiang L, et al. circ_0023461 Silencing Protects Cardiomyocytes from Hypoxia-Induced Dysfunction through Targeting miR-370-3p/PDE4D Signaling. Oxid Med Cell Longev 2021;2021:8379962.

20. Li Y, Shi R, Zhu G, et al. Construction of a circular RNA-microRNA-messenger RNA regulatory network of hsa_circ_0043256 in lung cancer by integrated analysis. Thorac Cancer 2022;13:61-75.

21. Li L, Sun D, Li X, et al. Identification of Key circRNAs in Non-Small Cell Lung Cancer. Am J Med Sci 2021;361:98-105.

22. Zhang J, Liu Y, Shi G. The circRNA-miRNA-mRNA regulatory network in systemic lupus erythematosus. Clin Rheumatol 2021;40:331-9.

23. Zeng L, Zhang P, Fang Z, et al. The Construction and Analysis of Infiltrating Immune Cell and ceRNA Networks in Diabetic Foot Ulcer. Front Endocrinol (Lausanne) 2022;13:836152.

24. Du J, Zhang L, Zhuang S, et al. HDAC4 degradation mediates HDAC inhibition-induced protective effects against hypoxia/reoxygenation injury. J Cell Physiol 2015;230:1321-31.

25. Oliveros JC. Venny. An interactive tool for comparing lists with Venn's diagrams. 2007-2015.

26. Aggarwal S, Randhawa PK, Singh N, et al. Role of ATP-Sensitive Potassium Channels in Remote Ischemic Preconditioning Induced Tissue Protection. J Cardiovasc Pharmacol Ther 2017;22:467-75.

27. Yin L, Tang Y, Jiang M. Research on the circular RNA bioinformatics in patients with acute myocardial infarction. J Clin Lab Anal 2021;35:e23621.

28. Guo Y, Luo F, Liu Q, et al. Regulatory non-coding RNAs in acute myocardial infarction. J Cell Mol Med 2017;21:1013-23.

29. Zhai C, Qian G, Wu H, et al. Knockdown of circ_0060745 alleviates acute myocardial infarction by suppressing NF-kappaB activation. J Cell Mol Med 2020;24:12401-10.

30. Hu X, Ma R, Cao J, et al. CircSAMD4A aggravates H/R-induced cardiomyocyte apoptosis and inflammatory response by sponging miR-138-5p. J Cell Mol Med 2022;26:1776-84.

31. Wang J, Cai H, Liu Q, et al. Cinobufacini Inhibits Colon Cancer Invasion and Metastasis via Suppressing Wnt/β-Catenin Signaling Pathway and EMT. Am J Chin Med 2020;48:703-18.

32. Sun LY, Zhao JC, Ge XM, et al. Circ_LAS1L regulates cardiac fibroblast activation, growth, and migration through miR-125b/SFRP5 pathway. Cell Biochem Funct 2020;38:443-50.

33. Wang Q, Liu B, Wang Y, et al. The biomarkers of key miRNAs and target genes associated with acute myocardial infarction. PeerJ 2020;8:e9129.

34. Navickas R, Gal D, Laucevicius A, et al. Identifying circulating microRNAs as biomarkers of cardiovascular disease: a systematic review. Cardiovasc Res 2016;111:322-37.

35. Cheng M, Yang J, Zhao X, et al. Circulating myocardial microRNAs from infarcted hearts are carried in exosomes and mobilise bone marrow progenitor cells. Nat Commun 2019;10:959.

36. Fan PC, Chen CC, Peng CC, et al. A circulating miRNA signature for early diagnosis of acute kidney injury following acute myocardial infarction. J Transl Med 2019;17:139.

37. Shi J, Bei Y, Kong X, et al. miR-17-3p Contributes to Exercise-Induced Cardiac Growth and Protects against Myocardial Ischemia-Reperfusion Injury. Theranostics 2017;7:664-76.

38. Yuan T, Yang Z, Xian S, et al. Dexmedetomidine-mediated regulation of miR-17-3p in H9C2 cells after hypoxia/reoxygenation injury. Exp Ther Med 2020;20:917-25.

39. Poulter JA, Ali M, Gilmour DF, et al. Mutations in TSPAN12 Cause Autosomal-Dominant Familial Exudative Vitreoretinopathy. Am J Hum Genet 2016;98:592.

40. Yang Y, Sun Y, Wu Y, et al. Downregulation of miR-3127-5p promotes epithelial-mesenchymal transition via FZD4 regulation of Wnt/beta-catenin signaling in non-small-cell

lung cancer. Mol Carcinog 2018;57:842-53.

41. Strakova K, Matricon P, Yokota C, et al. The tyrosine Y250(2.39) in Frizzled 4 defines a conserved motif important for structural integrity of the receptor and recruitment of Disheveled. Cell Signal 2017;38:85-96.

42. Zhou X, Jiang J, Guo S. Hsa_circ_0004712 downregulation attenuates ovarian cancer malignant development by targeting the miR-331-3p/FZD4 pathway. J Ovarian Res 2021;14:118.

43. Zhang G, Liu Z, Zhong J, et al. Circ-ACAP2 facilitates the progression of colorectal cancer through mediating miR-143-3p/FZD4 axis. Eur J Clin Invest 2021;51:e13607.

44. Yin C, Ye Z, Wu J, et al. Elevated Wnt2 and Wnt4 activate NF-kappaB signaling to promote cardiac fibrosis by cooperation of Fzd4/2 and LRP6 following myocardial infarction. EBioMedicine 2021;74:103745.

(English Language Editor: L. Huleatt)

Table S1 The 191 DE-circRNAs screened from the GSE169594 dataset

ID	adj.P.Val	P.Value	t	B	logFC	SEQUENCE
ASCRP3010807	0.519	0.0049996	3.831635	-1.8988	5.3093478	TACTTGCGCTGCATGTGCCATAGGCCCATTTGAGTATTTTGTTTTCAATTAGGGAGATAG
ASCRP3004792	0.519	0.0035226	4.081286	-1.6407	4.5748006	CATGTGCCATGTCGCCTGGTTCTAGGAATAATGGGGGAAGTATGTAGGAGTTGAAGATTA
ASCRP3012480	0.519	0.0044896	3.907665	-1.8189	3.8901036	TGGGCCATACGGTAGTATTTAGTTGGGGCATTTATGTGATTAGGAGTAGGGTTAGGATGA
ASCRP3000368	0.473	0.002252	4.410168	-1.3193	2.9176593	AACAATCACCAGGCTCGGGTTATGTATGATTTTGCTGCTGAACCTGGAAATAATGAACTG
ASCRP3001027	0.561	0.0111901	3.279208	-2.5109	2.7838779	ACAAGTTGGATATTCCAATGTTCTTTGTGGTTTTTGGCAAATTTGTCATATCAAGAAGCA
ASCRP3001166	0.941	0.2428758	1.26082	-4.9031	2.5398629	ACAGTTAAAGAAGAAATCTGAAGAGGAAAAGAATGAAAAGATAAGGAGTCTAGAAACCAA
ASCRP3003503	0.561	0.0112289	3.276892	-2.5136	2.2582307	CAACAACCGCTTGGAATGCTGCAACAATGACTTAATTCAGTGCACAAATGAGATGAATGT
ASCRP3000495	0.578	0.0169489	3.004203	-2.8344	2.0646497	AACTCTTACTTACATGTCTCATCGAAACTCCAGAACAAACATCAAAAGAGCCAACACAGA
ASCRP3001059	0.656	0.0269642	2.70221	-3.2006	2.0490843	ACACCAGGAAAGAAAAAATGCCTGTCTTAAAGGCTGAAGCGTCACATTATAACTCTGACT
ASCRP3012300	0.473	0.0006761	5.359988	-0.5068	2.0416799	TGGACAACAGAAGACTGGACTGAAGATAACTGGCATCAAATACTCACAACATAGCTCAGG
ASCRP3011209	0.473	0.0005485	5.536109	-0.3741	2.0335632	TCAGAGCCTGAACTGGCATCAAATACTCACAACATAGCTCAGGATCTGTCAAACAAAAGT
ASCRP3004521	0.544	0.0075895	3.541949	-2.213	2.0099575	CATAAAGGCAGCTTTGAAACACTCCTAAAAGACGACGGCCTGCACGTTCAATTTTTGATG
ASCRP3007020	0.544	0.006712	3.626392	-2.1198	2.00225	CTTCGGGGAGGTGAGTTCCCAGAGAACGGGGCTCCGCGCGAGGTCTGAGACTAGGGCCAG
ASCRP3013169	0.561	0.010291	3.335393	-2.4462	1.9904484	TTGAGCGCATTGCATCACATGATTTTGACCCCACAGGTTTCCCCTCAAAAAACCTATAAG
ASCRP3011287	0.57	0.0156763	3.055496	-2.7732	1.9660615	TCATGATCATCATAGGAGTGGAGAACATGCACAAGTCAACTTTGTAGTGTGCCAACTCTT
ASCRP3008499	0.575	0.016398	3.025894	-2.8085	1.9343917	GATATGGGATGAGAAAGTTCAAGTCAACTTTGTAGTGTGCCAACTCTTTGCCTTGCTAGC
ASCRP3006957	0.473	0.0005334	5.559908	-0.3565	1.8954451	CTTCAGCGGATTTGGGGATTAGGCTCTTTTAGGAGAAGTACAGCATCGGGGAGCCCACAG
ASCRP3002800	0.473	0.0010684	4.986563	-0.8062	1.8926314	ATCATGGTCCTGGGATACCTCAGACAATGGCAGCTTTTGGATTGAAATATTTGCTGAATG
ASCRP3011131	0.575	0.0164536	3.023671	-2.8111	1.8150551	TCAAGAACAGTAAAGTTGGAACACAGCAGAGGGTGTGTAATAAAATACAGCGTGACGACA
ASCRP3011389	0.567	0.0144713	3.10824	-2.7107	1.813903	TCCCTGAGCTTCGGGGAGGTGAGTTCCCAGAGAACGGGGCTCCGCGCGAGCTCATCAGTG
ASCRP3012020	0.564	0.0135939	3.149624	-2.662	1.7813205	TGATTTGATGCATAAAGGCAGCTTTGAAACAAAGAAGTTCGTGCCCCAATTCCTCAAAAG
ASCRP3000074	0.567	0.0149145	3.088324	-2.7343	1.7778091	AAAAGCAGGAAATACTGGTGGAACCAGAACCATTATTTGGTGGTGCAAGTGAAAGTGTAG
ASCRP3001047	0.473	0.0015016	4.718806	-1.0367	1.7769406	ACACACCATCATGGGATACCTCAGACAATGGCAGCTTTTGGATTGAAATATTTGCTGAAT
ASCRP3007104	0.473	0.0014478	4.747132	-1.0117	1.764434	CTTGGAAGAATTCTGTGGAAGAGTGGACAACAGAAGACTGGACTGAAGATGATTTGGACG
ASCRP3001875	0.561	0.0104385	3.325826	-2.4572	1.7609216	AGAGCGAGAAAGAAAAACAGCTGGAGACCCTGAAGGAAGATTGGGAATCTGAAAAAGATT
ASCRP3004864	0.561	0.0131517	3.171556	-2.6362	1.7499806	CATTGATTTGATGCATAAAGGCAGCTTTGAAACAAGAAGAAGTTCGTGCCCCAATTCCTC
ASCRP3003552	0.561	0.0121473	3.224393	-2.5745	1.7307824	CAACCAAAGGTTGCACCAACAACCGCTTGGAATGCTGCAACAATGGATTCACTCCTTCTC
ASCRP3011746	0.703	0.039852	2.451031	-3.5107	1.7126169	TGAAAGGAGAGCAAGAATCTCATAGAGCCAACACAGATCTATAGATTTCTTCGAACTCGG
ASCRP3009450	0.519	0.0050649	3.82251	-1.9084	1.7062885	GGAGACAGACGGAAGTGTTTGGATTGTGAGCTATTTCAGAACTGTTCTCAGGACTCATTA
ASCRP3005460	0.715	0.0432452	2.398671	-3.5756	1.695885	CCTGCTTAAAAAGGCCAAGGTGCTTTTCAGTGGGAAGAATTGGAAGAAGATATCAGGAAG
ASCRP3002176	0.519	0.0045459	3.898821	-1.8282	1.6941942	AGCTTGGAACAGACTCACGGCCAGCGAACTGAGTGCGTCCTGTCACTCCACTCCCATGTC
ASCRP3001182	0.519	0.0039796	3.993568	-1.73	1.670152	ACATCAAGACAGGGGGAAGAGTTTATGGAACTACAGAAAGTGACTGAGACCGAAGATGAT
ASCRP3003062	0.606	0.0197106	2.90547	-2.953	1.6687446	ATGGACAATATTCTGCTGATTTTTCAGGGTCAACTTTGTAGTGTGCCAACTCTTTGCCTT
ASCRP3006961	0.524	0.0058508	3.72157	-2.0163	1.6495081	CTTCAGGGAATTTTTTGGTGGAAGGGACCCATTTTCATTTGACTTCTTTGCCACCACCAG
ASCRP3013073	0.55	0.008732	3.446363	-2.32	1.6108931	TTCTCACCCCGGAAACATTTCTTTGATTGTCTTTGGCATCCTGAAATCTCTGGCCCAATA

Table S1 (*continued*)

Table S1 (*continued*)

ID	adj.P.Val	P.Value	t	B	logFC	SEQUENCE
ASCRP3009804	0.519	0.0050278	3.82768	-1.903	1.5988908	GGTGGAAGGGACCCATTTTCATTTGACTTCTTTGCTAAGAAACGGGACATCTATGACAAA
ASCRP3000221	0.473	0.0013938	4.776714	-0.9857	1.5966101	AAAGCTAGTAGTTTGGGAAGCTGCTCAGAATGGTGCAGATGAGGGAACTGGATTTGGACG
ASCRP3007103	0.544	0.0068786	3.609491	-2.1384	1.5800247	CTTGGAACAGACTCACGGCCAGCGAAGTGAGTTCAATGGCTGAGGTGAGTTCCCAGAGAA
ASCRP3010480	0.473	0.0018875	4.54333	-1.1951	1.5774205	GTTTGAGGAAGAAAAGGTGAAACGGCAGAATGAAATCGCCAAGAAGCGGAAAAATCCAAG
ASCRP3001842	0.817	0.0721613	2.070384	-3.9814	1.5607868	AGAGAAAAACAAAAGGCTTGTGGATCAGAATCTGAACAAAATTGGGAAAGATGAAATGCT
ASCRP3006434	0.603	0.0190569	2.927481	-2.9265	1.5583473	CTGAAAGAGCCAAATCGGATGAGTCCATCAAGGAAGAAGACAAAGACCAGCTGAACCTTC
ASCRP3000384	0.544	0.0074324	3.556278	-2.1971	1.5577644	AACAGACTCACGGCCAGCGAAGTGAGTTCAATGGCTGAGGTGAGGTGAGTTCCCAGAGAA
ASCRP3005749	0.715	0.0425227	2.409465	-3.5622	1.5525202	CGTGCTGTCGTGCAGGAGAAGGAAAGGAGGCTGAAGGGTACATCCGGGAAGGCTTCCTGG
ASCRP3000038	0.788	0.0618827	2.169087	-3.86	1.550489	AAAACAAAAGGGAGGCTTGTGGATCAGAATCTGAACAAAATTGGGAAAGATGAAATGCTT
ASCRP3010923	0.786	0.0602903	2.185808	-3.8393	1.5490367	TATACAATCTGTCACCTAAGTCTTATCGAACTGCCAAGTTTCACAGCCGGGTGCCTCATC
ASCRP3012178	0.606	0.0196121	2.908737	-2.9491	1.5462704	TGCTAACAAAAACAGAACTTTTTTAGAAAATATGCACCAAGTGAGAATGGGCCAAATGGG
ASCRP3003066	0.561	0.0105839	3.31654	-2.4679	1.5302793	ATGGAGAAAAGGGACAGTATACGCACAAAATTTATCACCTAAAGAGCCGTGTGGTTTTGC
ASCRP3001025	0.715	0.0429672	2.402803	-3.5705	1.5253169	ACAAGTCGATGGATTCCTCTCATAAATGAAAGAACAGACAAAGACAGCAGGTTCCTCCCC
ASCRP3003030	0.556	0.0091532	3.414432	-2.3561	1.5248933	ATGCCTCCTTTGCCGGAGCTTGGAACAGACTCACGGCCAGCGAAGTGAGTTCCCAGAGAA
ASCRP3003727	0.64	0.0240664	2.775726	-3.1106	1.5134604	CAATCAAAAGGGAAATCCTCATTGACGATTCAATTTGTTGAAGGCCAATTTGTGGACTCC
ASCRP3011118	0.539	0.006496	3.648983	-2.0951	1.496404	TCAACCTAGGGAAGAAAAACCTGATAGTAAGAAGGTGGAGGAAGACTTAAAGGCAGACGA
ASCRP3005233	0.517	0.0032866	4.131488	-1.5903	1.4917572	CCCTATATTTTAGAGCATCTGGAGGTCACTCTGTGAGACTGCTGGGTCAGAAAAAGGATA
ASCRP3009663	0.519	0.0038343	4.020238	-1.7027	1.4916239	GGGAAGATGATTCAGATGAAGACATGTCTAATTTTGATCGTTTCTCTGAGGCAGCCTGCT
ASCRP3006932	0.615	0.0211446	2.859733	-3.0084	1.4892996	CTTCAACTTGTAGACACAGCCGGGCAAGGAAATCCTCATTGACGATTCAATTTGTTGAAG
ASCRP3010386	0.473	0.0022178	4.421622	-1.3084	1.4873594	GTTCTCCTCAGAGCCTGGATTTGGACGTGGCAGAGGGAGAGGGGCAGGAAGGTTCTCAAC
ASCRP3012595	0.517	0.0028889	4.225619	-1.497	1.4778131	TGTCAGGTGGGAGAAAGCATTAACAACAGTGTCTTCAGTGTTCGCTTTTTCAGAACTACA
ASCRP3012188	0.66	0.0285281	2.665836	-3.2453	1.4579081	TGCTCAGAGAGTAATGCTCCTTCAACAAGGTCTTAATGACAGATCAGCATATGCTACTTT
ASCRP3011768	0.561	0.0132653	3.165848	-2.6429	1.4546996	TGAACTAGTAGATAGAGCCAAACAATCTTTTCAAGGTCACTCTGTGAGACTGCTGGGTCA
ASCRP3008643	0.82	0.0755003	2.041265	-4.017	1.4526748	GATGATTTATTAAGAGCTCAGCAAAACAGTCCCTCATCTACGGGATCTGGCAACACAGAG
ASCRP3012762	0.564	0.0135296	3.152769	-2.6583	1.4451515	TTAAACGGCACCAGGTGCCCAGATGACTATCATGAGCCAAGCTTGTGCAGAAAGGTGTAA
ASCRP3005983	0.519	0.0050481	3.824839	-1.906	1.4441595	CTATAGGAGACATTAAAACGGGAGCACCACAGTATGGTGCTAATCCTCCATCTGGAATTG
ASCRP3000693	0.561	0.0114768	3.262288	-2.5305	1.4355288	AAGGGACCCATTTTCATTTGACTTCTTTGGACCCATTCCAACAATCTCGTAAAACATGGT
ASCRP3000292	0.567	0.0139276	3.133566	-2.6809	1.4185635	AAATCAGCAGAGGATGCAGGCAACAGAACATTGAGGAAAACATGACAATAGCTATGGAAG
ASCRP3010200	0.949	0.375175	0.939037	-5.1959	1.4153788	GTGCTTTGTGGTGTACTGAAATCATGTCTAAGAACAGAGAACTTAACACCACCGTGCCTG
ASCRP3003016	0.817	0.0719367	2.072388	-3.9789	1.413512	ATGCATCATTGTGCGTCCCTGTATGCATACTACCTTGTACTGGTTGAAGAAATATGGAGA
ASCRP3009291	0.473	0.0008283	5.19227	-0.6382	1.4123722	GCTTGAGAAGAGATAAAGTAAAGGGTTTGAAAGTATTCTTGAAGGGCTGTTTGGACCTGC
ASCRP3007442	0.804	0.0676012	2.11235	-3.9299	1.3930022	GAACAAGCAGTTCAAGTGGAAGGAGGCAAAACCGGAAGACCTTATGGATTCAAAACTTAG
ASCRP3003345	0.546	0.0076788	3.533947	-2.2219	1.3915329	ATTTCTGGTCTCATCTACGAGGAGACTCGCGGGATTTTTGCGGCTATTTTCGTTGGTGTG
ASCRP3002278	0.945	0.3231127	1.05293	-5.0992	1.3796339	AGGCAGAAAAAATAAAGAGGGTTGATTTCTTTATTCCAGGAGTCTCTGTGGTTGGTGGGT

Table S1 (*continued*)

Table S1 (*continued*)

ID	adj.P.Val	P.Value	t	B	logFC	SEQUENCE
ASCRP3000608	0.561	0.0103904	3.328933	-2.4536	1.3738279	AAGATGAAGATGGCTGGGCTGAACGCCATCCAGACTCTCGATTCCTTCCTTGGGCTTTTC
ASCRP3008889	0.567	0.0143379	3.114361	-2.7035	1.3725745	GCACATGGCAGGATGAAGGAAAAAGAAGCAAGATCTAAATTTAGACAGTGAAGTTATTCG
ASCRP3009264	0.473	0.0024355	4.351732	-1.3748	1.366045	GCTGTAGACTACGAGGGCTCCAGAACCCAGGAAGATTCTTCTAACAGAGAAAATGCCATT
ASCRP3012532	0.473	0.0016124	4.663808	-1.0857	1.3563413	TGGTGGATCAGCTTTTCTGCAAAAAATTTGACATGAGCTTCTGAATTCAACACGTGAAGA
ASCRP3001758	0.704	0.0406382	2.438511	-3.5262	1.3560458	AGAAGTTCGTTGGAAGCAAAAAAAGCCCAGTGGAGGAAAGAGCTAGGTCAATATAGTCTA
ASCRP3011363	0.609	0.0206808	2.874166	-2.9909	1.3374739	TCCATTATTGGGAAATGTCAAGCCTAGAGGCAACCAAAAACATGGTGCATCCTTTATCAT
ASCRP3004458	0.594	0.0180962	2.96129	-2.8858	1.3337678	CAGTGATATGGAGAATTGGCCAACACCAAGTGAATTAGTGAACACTGGAAATTCGGTTCC
ASCRP3000659	0.787	0.0605983	2.18254	-3.8434	1.3325454	AAGGAACGATCTCGTAAGAAGGATTCAGAACACCTTTGTCCTAGAATATTGTGGAGAGGT
ASCRP3001922	0.659	0.0279516	2.679	-3.2291	1.3320186	AGATCAGAATCTCAGTCCAACAAAAGGTTGTTCTTTTAAAGAATTATTGAAGACGAAGGT
ASCRP3010719	0.672	0.0313344	2.605413	-3.3197	1.331423	TACATGCCCAAGAGGGGACTTGATGTTAACAAATGTGAGATTGCCAGAAAAATATGCAGG
ASCRP3012242	0.561	0.0126121	3.199394	-2.6037	1.3283037	TGCTTAGAAGCACATGGAAAAAAGGCTGAGAATTTTTTCTCGTGGATCTTTGTTTTGCTC
ASCRP3004884	0.679	0.0330782	2.570588	-3.3627	1.3259095	CATTGTTGGGACATGTATATTGTACACTCAGAAGAAGCCTTGTTTTTACTGGCAACCTGT
ASCRP3000596	0.659	0.0280194	2.677439	-3.231	1.3198202	AAGAGGCAAAACTTCGGACATAGAGGCCAACCAACCTTTGGAGAGTGAAGAGAGAACCTG
ASCRP3004163	0.546	0.0079998	3.505959	-2.2531	1.3149378	CAGAGCTTGGAGACAGACGATGCACACTTGACTGAAGGAGGACAGGGAATCTGAAGACTC
ASCRP3009451	0.817	0.0728506	2.064267	-3.9889	1.3144459	GGAGACAGAGAATTCTGCTTGGTCAGAATCGTGATGGCATTGTGTTCAGCACTGATGACT
ASCRP3002350	0.721	0.0450921	2.371883	-3.6088	1.3143359	AGGTGTCAGGGCAGAAACCAACAAAGAGTGATGACAGACCTAATGCTCTATTAAGTTCAC
ASCRP3009813	0.852	0.103165	1.839076	-4.2615	1.3141351	GGTGGTGATGGAGGTGGAGAGCATTAAACTGTCTGCACTGCAGCTCTCACCTGCTGATTG
ASCRP3013248	0.546	0.0084243	3.470741	-2.2926	1.3058494	TTGGGCCTTTCTTTTTATCAGCCTCCAGAAGGGGATAATGCACATGTGTATATCTCATGA
ASCRP3000071	0.517	0.0033068	4.127053	-1.5947	1.3055915	AAAAGATTCAGAGTTGGATAAGCACTTGGAATCACGGGTTGAAGTCGAGATAACATGAGT
ASCRP3008101	0.679	0.0334619	2.563178	-3.3718	1.3039748	GAGACAAGCAAATCTGACAGGATGGCATCTGATGACTTTGACATAGTGATTGAGGCCATG
ASCRP3002787	0.473	0.0016891	4.628102	-1.1178	1.3014059	ATCATATAACTAGTGTGAGGAGAGGTATCTTATTGACAGCCGGTGGTTCAAGCAGTGGAA
ASCRP3008256	0.62	0.0219135	2.836515	-3.0365	1.2910984	GAGCTCTGACTGCAGACCTACCAAAACAGTGGAAGAACTCAGAAACAACTAGTAGATTAT
ASCRP3008176	0.813	0.0696848	2.092842	-3.9538	1.2902047	GAGATACCTTAGCCTGGCCTACAACAAGAGGTTGTGTTTTCATCTTACCCTGGATTTTCA
ASCRP3007913	0.603	0.0192318	2.921515	-2.9337	1.2901266	GACCCATTTTCATTTGACTTCTTTGATATCGGAAACTGGCACTGAAGTGGCATCCAGATA
ASCRP3000615	0.519	0.0042011	3.954893	-1.7699	1.2778444	AAGATTCAGAGTTGGATAAGCACTTGGAATCACGGGTTGAAGGGAAGTCGAGATAACATG
ASCRP3012497	0.473	0.000404	5.80014	-0.1848	1.2766017	TGGGTGGTGATGAGGATGTAGATTTACCAGAAGTAGATGGAGCAGATGATCTTAATTGGC
ASCRP3011981	0.561	0.0118955	3.238358	-2.5583	1.2763166	TGATGAGAATACTTCCATCATCTTTAGACCTAACTCAAAGAGAGACATCTCCCCATACAT
ASCRP3009699	0.831	0.0811202	1.994973	-4.0735	1.2732434	GGGATTCTGACCATCTCACATGCCACATTTCTTTCAAGATGGCTTGAAAACAGCTGATAA
ASCRP3004184	0.703	0.039459	2.457385	-3.5028	1.2729753	CAGAGTGATGAACAACTTCATCAAGAAATATCTCAGGTTCCTCCCCGGGCAGAAGAAATC
ASCRP3006285	0.942	0.2586472	1.215928	-4.9474	1.2705532	CTCGCAGTGGGGGAGATGGAGGTGGAGGAGAGAGATGCTGTGTGGGGGTGCGGGTTCCTT
ASCRP3013230	0.72	0.0444242	2.381441	-3.597	1.2670731	TTGGAGTTGGAGACAGGCACCTGGATAACCTTTTGCTAACAAAAACAGGTATGTGATAGT
ASCRP3003651	0.763	0.0557217	2.236318	-3.7769	1.2643571	CAAGCCTGGTTCAGTTAAACCTACTCAAACTATTGAGGCTGCCTCCATTCGAAACATTTT
ASCRP3005568	0.544	0.0069704	3.60036	-2.1484	1.25518	CGAAGTGAGTTCAATGGCTGAGGTGAGGGGCCCGGCGGATGCCTCCTTTGCCGGAGCTTG
ASCRP3008212	0.473	0.0015864	4.676326	-1.0745	1.2515241	GAGCAACTTGCTAATGGCAGGCATTTTACAAGGATGGGTCATCAGTTAAGGAAGTTGAAA

Table S1 (*continued*)

Table S1 (*continued*)

ID	adj.P.Val	P.Value	t	B	logFC	SEQUENCE
ASCRP3010151	0.674	0.0316197	2.599582	-3.3269	1.2450144	GTGAGCATTACAGATTGTGCTTCAAGAAGACCATAGGGAAGAACGCATTTTCATCTTGCT
ASCRP3009594	0.713	0.0422318	2.413863	-3.5568	1.2377446	GGCCTCTCAGGATGAAACAAGTGAAGATGCTAACTGTCTTGCTTTGAGTGGACATGATAA
ASCRP3008027	0.85	0.0972081	1.877797	-4.2152	1.2351698	GACTTATCATGACCTCAGACTATCAGCTTCAGAAGCTGCTTACCATGGACCCAATAAAGC
ASCRP3004906	0.645	0.0243345	2.768551	-3.1193	1.2295075	CATTTGGAGGAGCAACAATGTGGGACTATACGGCACCATACTGGACATACCTTTTATGTG
ASCRP3011267	0.473	0.00169	4.627693	-1.1182	1.222671	TCATATAACTAGTGTGAGGAGAGGTTGAAGGTATCTTATTGACAGCCGGTGGTTCAAGCA
ASCRP3002609	0.688	0.034307	2.547156	-3.3916	1.2151294	ATACATATCACAACACAGGGCTACAGGGGAAGAATTGAAAGTGAAGGCATACCTACCAAC
ASCRP3012185	0.647	0.0251128	2.748178	-3.1442	1.2108112	TGCTATTGAGTTAAATGCAGCCAATTATACAGTGTGGGACAGAGCAGAATGGGCTGATAT
ASCRP3004883	0.837	0.0843709	1.969595	-4.1044	1.2085869	CATTGTTGGGACATGTATATTGGCTGCTATATGGCAAGCACTAAACCACTATGCTTACCG
ASCRP3007605	0.723	0.0455707	2.365121	-3.6172	1.2078575	GAAGCCAAGATGACCAGAATGTTTTTAAATAATCCCGTGACGACAGCATGTACGATCCCT
ASCRP3011803	0.758	0.0522858	2.27709	-3.7264	1.2051551	TGAAGGAGATGAAGTAGAGGGATTTATCAAAGATGTTCATGAAGACTCCCTTACAGTTGT
ASCRP3003414	0.844	0.0925976	1.909352	-4.1772	1.1996936	CAAAAGTAAAATTGGCAAGACATATCCTTACAGGCAGAGAGCACACGTCACATGGAGATG
ASCRP3003295	0.594	0.0180661	2.962379	-2.8845	1.1946383	ATTGGGGGATCTGGACCGAGTCAAGTCAAAGGAAGCAAAAGAAGACCTGATATTGAATAG
ASCRP3001122	0.914	0.1781996	1.475844	-4.678	1.1941129	ACAGCACAGTCAGCCAGCCTAATCTTAGAACCACAGTAAAATGATTTAGCTTTGGAGTCA
ASCRP3011877	0.84	0.0909617	1.92091	-4.1633	1.1888035	TGACTGGTGAATTTGAGAAGAAGTATGTAGCTTGTATTGGTTGGTGATGGTGGTACTGGA
ASCRP3008387	0.721	0.044894	2.374704	-3.6053	1.1823348	GAGTAACTCTGTCCTTATTATCGGACCCCGAGGATCAGGAAAAACTATGGAAGCCTGGAG
ASCRP3006148	0.689	0.0362532	2.511731	-3.4355	1.1792042	CTCATCCACACCGTGTTGCTGCAAAAGGACTATCAGGACATATCCAATGATGATGATGAC
ASCRP3011166	0.519	0.0039038	4.007351	-1.7159	1.1784074	TCACAGCACGGTGGAGGAACTGCAATGTCTGGTGGAGAACAGAAACCAGAGAGGTACTAT
ASCRP3004489	0.78	0.0592311	2.197172	-3.8253	1.1736561	CAGTTACGGCAGGAGGCCGAGCAACTTAAGAACCAGATTCGAACAAATTTACATGTATTG
ASCRP3013220	0.631	0.0232299	2.798652	-3.0826	1.1709952	TTGGAAATGAACAGATACCAAACTTGCCAGTAGGGAGAAGGGAAAGTTTTGCTTTAAGGC
ASCRP3010462	0.801	0.0669779	2.118301	-3.9225	1.164908	GTTTCCAAGCAACAATCAGTGCTCCACACATGAAAATGGAATCATCAAGACAGATAAAGT
ASCRP3009698	0.862	0.1116302	1.787548	-4.3226	1.161836	GGGATTCTGACCATCTCACATGCCACATACAAAAATTGAGAAAGAGAAAAGAGAGCACGC
ASCRP3005075	0.875	0.1187717	1.746862	-4.3705	1.1603568	CCAGTAGCACCAGGATATGTCTTTTCCAAGATGAGATGGGATTCTCCAACATGGAAGATG
ASCRP3013124	0.852	0.1039268	1.834278	-4.2672	1.1593692	TTCTTCCAAGGAACCAGTGCGAAGCAAAGAATGGCTCAAGAAGTACTGACACATTTAAAG
ASCRP3000180	0.66	0.0282743	2.671599	-3.2382	1.1545939	AAAGAAAGAGGTCTAGAAGTACCTAAACCTGGTTGGACCGACAGTTACAAGACATAGTGT
ASCRP3003327	0.679	0.032882	2.574413	-3.3579	1.15418	ATTTAGGAGGATTCGATGGCAATTTTTTGTGGAACAGAATTGGAGCAGTTTTGACGAAGT
ASCRP3013392	0.884	0.1247446	1.714556	-4.4083	1.150398	TTTCCTAGAAGCTTGCAGAAAAATTGGTGTACCTCAGAGTGATGACAGACCTAATGCTCT
ASCRP3009424	0.711	0.0417031	2.421934	-3.5468	1.1499299	GGACCCCGAGGATCAGGAAAAACTATGGATTTGAATTTGTTGAAATGAGCAGTCGTAAAT
ASCRP3001941	0.84	0.0864207	1.954073	-4.1232	1.1419647	AGATGAATTTACATGAACTTGAAGATGATTTACTTGGAGAAGATTTGCTATCTGGCAAAA
ASCRP3003469	0.584	0.0173514	2.988812	-2.8528	1.1408087	CAAAGTTCACCTGTTTAGCTACCCCTGCTGTCAGCCTCGAGGGACCCGGCTACCTGTAAG
ASCRP3012190	0.886	0.1282952	1.696027	-4.4298	1.1373508	TGCTCAGCAGGAGCTTCATCAACGATATATGTCAGATCTAAAGAACATTCTAGTATGCCA
ASCRP3003415	0.844	0.0936221	1.902212	-4.1858	1.1348366	CAAAAGTCCATTCAGAAAAGACAAGAGCCCTGTGAGGAGGAAAAAAAGCAAGAGCAGAAG
ASCRP3012365	0.609	0.0202947	2.886437	-2.976	1.1276538	TGGAGTCAAAGGAAAACTAGGCAGACTTCTGGGCATATTTGAGGTGCTGCTGGTGAGTAG
ASCRP3009567	0.939	0.2305787	1.297554	-4.8661	1.1252005	GGCAGCTGTGAGGGATATTCTTGAAGGAATTCAAAGCAAATAATACTTCAGACAGAAAGC
ASCRP3012771	0.544	0.0075873	3.54215	-2.2128	1.1208608	TTAACATTTGGGAGAAACACAGCCAGAAGGAAGTGTTTGGATTGTGAGCTATTTCAGAAC

Table S1 (*continued*)

Table S1 (*continued*)

ID	adj.P.Val	P.Value	t	B	logFC	SEQUENCE
ASCRP3013275	0.82	0.0741276	2.053081	-4.0026	1.1174958	TTGTCAGCTCATTTGCAGCTTACATTTTTGGTTTCTTCCACAAAAATGAGCCAACACAGA
ASCRP3010882	0.84	0.0883073	1.940097	-4.1401	1.1153562	TAGGTTCTCACCCTGATGAAAGCGGAAGCAAATTCCAGAGAGCACGTTTTCAATATCATA
ASCRP3009803	0.899	0.1481782	1.600276	-4.5396	1.1149504	GGTGGAAGATTCTTCCAAGGAACCAGTGCGAAGTAATCTATGCCAGCAATTATGACAATG
ASCRP3005082	0.84	0.0908251	1.921885	-4.1621	1.1148125	CCAGTGAATCAAGCCAAGACATATAGAGCAGGCAAGTTAGGAAATCAACATTGAATCCCA
ASCRP3002714	0.817	0.0716553	2.07491	-3.9758	1.1147817	ATATTCTGGAATCCCAGCAGTTTCTTTCTGTTTTTGCGAGGTACCAGCAACTTCAAGGTT
ASCRP3007198	0.844	0.0921818	1.912271	-4.1737	1.1143582	CTTTCTATGACCCTGACACCAGCATCATTTACTTATGTGGAAAGACACGATGAGGCGAGT
ASCRP3007816	0.84	0.0849277	1.965343	-4.1095	1.108846	GACACCTCAGGGAAGAGACTTCCACCTTAGGATAGTGTTGCCTGAAGATTTACAACTGAA
ASCRP3001605	0.909	0.1707762	1.50475	-4.6463	1.1045332	ACTGGTTTGCAGAGTCCAGATAACAAAGCTTTATTCGTCATTTCCATGTCAGACAATGGC
ASCRP3000703	0.75	0.0500927	2.304533	-3.6924	1.1032089	AAGGTGAAGATGATACCTTTCTAACAGCCCAAGACTGTGAATTGGAGAATCAAGAGGCAC
ASCRP3007888	0.915	0.1797218	1.47005	-4.6843	1.1023078	GACCACAGGGACCACCAAGAAGGCCCGGAGGATATTATACCATTTATTGATAAATACTGG
ASCRP3011766	0.875	0.1188549	1.746402	-4.3711	1.1015059	TGAACCTGAAACTTGGTGGAAATTTGATCCTGAAGAATTAGAAAAATGTCTTATGGTGAA
ASCRP3001251	0.84	0.0896985	1.929973	-4.1523	1.1009974	ACCAAGAATGGAAACAGCGAAGGATACAGCCTGTGCACATCCTGACTTCTAATAATCATG
ASCRP3001001	0.902	0.1560892	1.565422	-4.5789	1.0980611	ACAACCAAAAACAGAGCAGTGCTGTGTCTACTAGTGGGAATTTAAATGGATATTATACCA
ASCRP3009875	0.902	0.1558767	1.566337	-4.5779	1.0954795	GTACATCTACATGCATTTTGGGGAGGTCCCTGAGTGCCAGAGGTGGTGGTGTTGCTTATC
ASCRP3002480	0.672	0.0310123	2.612061	-3.3115	1.0941838	AGTGGGGAGAGGAGAAGATTTGACTTCTGAACATCCTTTGTTAGTTTATTTAGGAAAGGG
ASCRP3009724	0.84	0.0860366	1.956954	-4.1197	1.0914048	GGGGACCCCTGGCTGAAAGACAAAAATTGGAGGAATCAGACATCATTGATCTTGAGAAAC
ASCRP3001821	0.519	0.0046398	3.884343	-1.8433	1.0852521	AGACCTTTGTATGTATTTCTGGTGGTCGCATTCATATGTCAGTTTTAGGAAGGCTTGGGA
ASCRP3003280	0.72	0.0443571	2.38241	-3.5958	1.0831269	ATTGCATTCCAACAGCTCATTTTATGTTGCTTACAGCACTTAGAAATTGTTGATGGCCGG
ASCRP3006793	0.561	0.0106649	3.311423	-2.4738	1.0789356	CTGTCTTCTGCTGCTGGGGATATTACATTAGGAAGTGTTCATGGGTCAAAAATTGCATGT
ASCRP3005133	0.904	0.1591291	1.552454	-4.5934	1.0787899	CCATTGCAAACCTTATTAATCTCAGGGAACTGGATGTCAGCAAGAATGAATGTTGGCTCA
ASCRP3008716	0.615	0.0214373	2.850792	-3.0192	1.074051	GATGTCGTTTGGGGATTAAACTCTTTGTTTACTCCTCCCAAAGTGAAATGCCTGACCAAG
ASCRP3001024	0.75	0.050823	2.295263	-3.7039	1.0719808	ACAAGTATTTGAAGAATATGTTTCGTACGTATCAGGGAGCTCAAAGAGGCCCATGAAGCA
ASCRP3004998	0.892	0.1392794	1.64157	-4.4926	1.065198	CCACCCACTGAGCCCTCTAGTACTACTAGAGAGCACGTTTTCAATATCATAGGAGCATTT
ASCRP3002378	0.679	0.0326307	2.579344	-3.3519	1.0614764	AGTACCATAGGCATCCTTCATCAAAAAGCCATTTGACCGTGGAGAAGTAGAATCAATGGA
ASCRP3003138	0.901	0.1538644	1.575059	-4.5681	1.0566236	ATGTGGAAAATTTCCTAGAAGCTTGCAGAAAAATTGGTGTACCTCAGGTCATGCTTCACC
ASCRP3012455	0.55	0.0087527	3.444752	-2.3218	1.0564353	TGGGAAAGACCTTGATCCCAACAATGTTATCATTGAGTCTGGTCCATCGAACTCATATGT
ASCRP3011066	0.757	0.0517904	2.283187	-3.7188	1.0558664	TATTGGAGAGAGAAGTCCATTAGAGATGTTTATGATTACTTCCGAGCTGTCCTGCAGCGT
ASCRP3005524	0.886	0.1358766	1.658004	-4.4737	1.0558399	CCTTGCTGCAGCCTGTGCACGTCGGGCGTAGTTCGGCTTCACATCAACAGCTGGCTGGAG
ASCRP3008217	0.679	0.0330418	2.571298	-3.3618	1.0445863	GAGCAGATTCGCAAAGAACAAGAAGAGGAACGTGAGGGAACACAACAGTAGATGAGTTAA
ASCRP3003394	0.624	0.0226058	2.816318	-3.0611	1.0405662	CAAAAACCTTTGGACAGTCCAATGTCAACATTGCCCAGCAAGTGGCCGGTCTAATTGAAG
ASCRP3009475	0.834	0.0817193	1.990223	-4.0793	1.0404098	GGAGGAGGACGAAGGTTCGAGAACTTGTCTTGGACAATTGCAAATCAAATGATGGAAAAA
ASCRP3009472	0.73	0.0466572	2.350031	-3.6359	1.039105	GGAGGAAAGAAGACAAGAGAGAACGCAAACAGTTTGAAGCTGAGGATTTTTCGTCATTGA
ASCRP3000344	0.609	0.0204846	2.880373	-2.9834	1.0387766	AAATTGTTGACTTGCAAGATGATGAGGATTTCCAGATAGACACAGGTAATGAGAGGCCCT
ASCRP3009085	0.82	0.0761238	2.035968	-4.0235	1.0357955	GCCGAAGAGGAAAGTCTAGTACTCAATAAAGGAGATTGCTTTGCATAAATCCACCCCTGT

Table S1 (*continued*)

Table S1 (*continued*)

ID	adj.P.Val	P.Value	t	B	logFC	SEQUENCE
ASCRP3009119	0.82	0.0762097	2.035241	-4.0244	1.0354813	GCCTTACAGTTAGAGAATCTTTGGATTTGTTTAATATGCGGCCACATAGGATGTGGACGG
ASCRP3013116	0.561	0.0100858	3.348942	-2.4307	1.0346293	TTCTTATCGTGGAAGGCAACAGGTGTCACAGCACGGGGATTCCCATCGAAACGTCATCAT
ASCRP3002057	0.899	0.1480724	1.600753	-4.5391	1.0244404	AGCATTCATGTTCCCTCACCAGCTGTAAGTGATGACAGACCTAATGCTCTATTAAGTTCA
ASCRP3003288	0.561	0.011559	3.257515	-2.536	1.0243366	ATTGGAGACATAGAATTTCAGGAAATCTATCAAATGTGGAAGAAATTGGGACTTGCTCGT
ASCRP3000585	0.844	0.0945638	1.895716	-4.1936	1.0240109	AAGAGATAGGAACTCTTGGTTGGGATAAGGAAGAGACTTCCACCTTAGGATAGTGTTGCC
ASCRP3001979	0.567	0.0146935	3.098175	-2.7226	1.0231285	AGATTTGTTCCTAAATTTAAGGGTATTAATGGCATTCTTGCTGATGAAATGGGCCTTGGT
ASCRP3004131	0.791	0.0635069	2.152465	-3.8805	1.0201035	CAGACTCCAGATCTCACATTCTTGAAGGTGGCATTGAAGAGCACTAAGATCGGAAGATGA
ASCRP3010660	0.877	0.1202316	1.738828	-4.3799	1.0180942	TAATTGGAGCCTTGCTGGGTGAACAGCAGAGAATTTCAAAGGACCTTGCTAATATCTGTA
ASCRP3001643	0.572	0.0161335	3.036581	-2.7958	1.0162385	ACTTCATTGGCCACCTACAGAAACAAAATGTCAACAAATTGATGGGATCTCCCAGCCATC
ASCRP3002815	0.552	0.009046	3.42241	-2.3471	1.0158813	ATCCACTGAATATTGAAGCTGCAGAACATCATTTGCGGGACAAGCCTCCCAAAGTGAAAT
ASCRP3001354	0.815	0.0710038	2.080785	-3.9686	1.0135951	ACCGAAGACACTCATGAAGTAGATTCCAAAGCAGCTTTAATACCGAATAACAATACTTCT
ASCRP3007978	0.822	0.0781072	2.019391	-4.0438	1.0135023	GACTAGGGAGAATAATCATGGGCCAGACTGGGAAGAAATCTGAGAAGGGACCAGTTTGTT
ASCRP3008956	0.875	0.1184766	1.748498	-4.3686	1.0120037	GCAGTAGAAGAAGAACAAAATGGAGCTCTCTATGAAGGCAGAAGCTGAGGAAGATTGTCA
ASCRP3006278	0.84	0.0891063	1.934264	-4.1472	1.0089168	CTCGAGAGTGCGAGAAAAATAGTACATGATTACAGTCCGGGACCATGTCTGGAGAACTAC
ASCRP3003038	0.808	0.0687393	2.101623	-3.943	1.0046945	ATGCTAAGAACTGCTGGGAGGATGACATTTTCAGTTTAAATTCTCAACTGGCAATTGGCC
ASCRP3001093	0.75	0.0507711	2.295917	-3.703	1.0024137	ACAGAAGATTCATTGAATGGCACCTGCAGAAGCTTTTCATGCAACACCCAACACTTATAA
ASCRP3001496	0.84	0.0859625	1.957511	-4.119	1.001143	ACTACATATTCCAGATGGTGAAGACATTCAGTGAAGCTTGCCTGATGGTAAGGAAACCAG
ASCRP3011510	0.946	0.3270609	1.043819	-5.1073	1.0006857	TCGTCTTTCATTTCACCTCGGTGATTTGGTGCTTCTACGTGGTGGTGACGACAGTGAGAC
ASCRP3010264	0.958	0.4362323	0.819472	-5.2881	1.0003315	GTGGTGGAAGACCTCATTAACCACTATGTGGTGGTGTTTAGTTGGCGGATGGCATACCAG
ASCRP3013532	0.561	0.0107699	3.304849	-2.4813	1.0002576	TTTTCACACAGGCAGCTTTGGAAGAAGTAGAAGGTGATGTGGCAGAATTGGAACTAAAAC

Table S2 The 201 DE-circRNAs screened from the GSE160717 dataset

ID	adj.P.Val	P.Value	t	B	logFC	SEQUENCE
ASCRP3010200	0.0539	0.00156037	5.171972	-0.7335	3.568485	GTGCTTTGTGGTGTACTGAAATCATGTCTAAGAACAGAGAACTTAACACCACCGTGCCTG
ASCRP3010264	0.0496	0.00104129	5.566915	-0.3181	2.93845	GTGGTGGAAGACCTCATTAACCACTATGTGGTGGTGTTTAGTTGGCGGATGGCATACCAG
ASCRP3011155	0.1488	0.01249542	3.404048	-2.8919	2.722207	TCAATGTGTGTGTATCTATAAGCCACCCAATTAGCACAGTATCAAACACCATGTCTCCCA
ASCRP3008634	0.0526	0.00135574	5.307018	-0.5888	2.618589	GATGAGTATTTCCGGCAGCCTGTGGTGGTCTTGGTGAAGAGTAACAACCTGACGGACCGC
ASCRP3008722	0.0743	0.0033088	4.486855	-1.5112	2.210297	GATGTGCTTCTGAGGTGGGCTGTGGAATGCCATGTGTAATTACTATTATCAGCATCTAGA
ASCRP3009800	0.0535	0.00147775	5.223964	-0.6774	2.209227	GGTGCCTCAGGTGGTGGTCTGTCACGTGGTGGGCCAGGCTATTCAGTTCTTGGTCAGCGA
ASCRP3013178	0.0356	0.00054864	6.235167	0.3332	2.179865	TTGATGACCGCAGCAGGTGGAAGATGAGCTCAGCTCCCCAGTGGTGGTGTTCAGATTTTT
ASCRP3006645	0.0344	0.00048202	6.377007	0.4636	2.1508	CTGCTGTTACTGCAGCAGTAAAGGCTGGTGTTTGGAATGCTTTATCCTGCATATTATTCA
ASCRP3004068	0.2898	0.04989734	2.39663	-4.3069	2.142004	CAGAAATCAGATGAAGGCCACCCATTCAGTTGTTGACCTCCTGTACTGGAGAGACATTAA
ASCRP3011510	0.0526	0.00136323	5.301683	-0.5945	2.114352	TCGTCTTTCATTTCACCTCGGTGATTTGGTGCTTCTACGTGGTGGTGACGACAGTGAGAC
ASCRP3004813	0.3424	0.07350685	2.126526	-4.6908	2.09077	CATTACAACAGTGCCACCCAATCTTCGAAAACTGGATCCAGAACTCCATTTGTGAAATGG
ASCRP3002745	0.3875	0.09761008	1.929526	-4.9662	2.061463	ATCAAGGAATCAACATTTACCGAAAGCCACCCATCTACAAACAGCATGGCTCCACCGTTT
ASCRP3008204	0.0232	0.00020631	7.369615	1.306	2.057797	GAGATTGTGTGTGGATCGATGCATTTGCAGAAACAAAGATTGTGTGTGGATCGATGATGA
ASCRP3009643	0.2756	0.04401747	2.484675	-4.1812	2.045381	GGCTGGCGAGGATGGAATCCGACGTGGTAGGCCCAGAGCAGATACTGTCCGCGATTTAAT
ASCRP3008289	0.0268	0.00025977	7.088818	1.0796	2.029329	GAGGAAAAGCATCGTGCTCTTTGTTCTCAGGTGTTTGTGTGCAGATATGATACATGCTTC
ASCRP3000697	0.05	0.00113646	5.479838	-0.4077	1.98056	AAGGGGGCTTCACATGGTTTTAAAATGTGCTGCTGTGGTTTGACCTAGAGTACAAAATAG
ASCRP3000513	0.0208	0.00010212	8.28337	1.9845	1.97414	AACTTGACTGGAGATGTGTGTGCTGTGATGAGGAAGATGAAGATCCTGCCAAAGGTGATC
ASCRP3007654	0.0391	0.00066521	6.028453	0.1384	1.973591	GAAGTGACCGATTTCTAGTGTGTGTTGGTGATGGGGCCGCAGCTGGTTTACCGGGGATTG
ASCRP3005368	0.0783	0.00368315	4.393874	-1.6225	1.950645	CCTCAGGATGGTGGTGTTGGCATGAGGAAAGGAGGTATCTTCGAGGGACAATCTTCTTCT
ASCRP3012539	0.0661	0.00252616	4.725994	-1.2313	1.949464	TGGTGTTTGGTTTGGAACATTTTATTATGCAGCCTTGAAAAGCTGAAACCTATCAACACT
ASCRP3010265	0.119	0.00762441	3.790044	-2.3791	1.939782	GTGGTGGTGCTATTCCTCATGATCACAGCCTCTACATATGCAATAAGCTAGGATTGTGTC
ASCRP3009314	0.4562	0.13807729	1.687432	-5.2943	1.929025	GGAAAAGCCACCCAGAGAACCCGCAAGGCTGTCATTATTTGTATCAAAAACAAAGAATTT
ASCRP3012176	0.1379	0.01067655	3.525087	-2.7288	1.921477	TGCGTTGTTTGTAGGATGTGGAGCCACCCAAAATTTCAAGCACAAAAAACATTTCCATTA
ASCRP3002732	0.0706	0.00304117	4.560806	-1.4237	1.910812	ATATTTTTGACTCTTTTGTGGGTGGTGTCGGGTAGGCCTCGCAATGTATTCAAGTTACTC
ASCRP3006919	0.3749	0.09162077	1.97353	-4.9052	1.896975	CTTATGGATATGACCAGCCACCCACACAGAATATGCCTATGGGTCCTGGAGGGATGAATC
ASCRP3005758	0.018	0.0000308	10.063765	3.0888	1.886162	CGTGTGTGTGGCATGCAGCCATAAGTTAGAAGAAGAATTTGAGTGGCTAAAGAAATCTGA
ASCRP3007563	0.0222	0.00017641	7.565448	1.4587	1.883575	GAAGAGCTTAGGTGGTGTGGGAAGATCTGTCTGAGAAGAAACAAGAAAGCAAACAGGTAA
ASCRP3003019	0.0413	0.00071551	5.95157	0.0644	1.879577	ATGCATTAGCAGATTGATGAACATAGGATATGTGTGTGTGTAAGAAAACGACCACTCAAT
ASCRP3006692	0.0551	0.00163183	5.129434	-0.7796	1.823261	CTGGATGAACGGAAATCTCCTGTGGTGGCAGTTGAGAAATGCTATGGTGAATCGAAAGAC
ASCRP3009152	0.3355	0.06998078	2.160691	-4.6426	1.810901	GCGGCTGGCGTCAAAAAGGCCAAGAAGGCTGCAGGGGCGAAAAAGGCAGTGAAGAAGACT
ASCRP3009642	0.3576	0.08090321	2.05993	-4.7845	1.804669	GGCTGGCAGGCAACACCTTAGGGTTACGAGAAGTTTCTGAGAAGCTGAACAAATATAATT
ASCRP3000492	0.1926	0.02116716	3.009729	-3.436	1.797755	AACTCCCGTGGCAGGTTGCATCTGCACTGGAGAAATGGAAGACAGCAATCCGGGAAGCTC
ASCRP3005316	0.0845	0.00413829	4.294036	-1.7436	1.797068	CCGTAGTGGATTGGTGGTTGGTGCAGTGGAGATGCCATTTCCAGTGTTGAACGATATGAT
ASCRP3010909	0.1998	0.02272988	2.957626	-3.5091	1.773051	TATAACCAGTTGGCTTTGCTGGCAGTGTATACGGTAAAATATGCCTTGATCAGTGCCCAG
ASCRP3013614	0.0179	0.00001707	11.059355	3.6037	1.759295	TTTTTTCATGATGTGTGTGGCAGAGAGAACATATAAACAGGAGGCTTTTAGGCGTTTGGG

Table S2 (*continued*)

Table S2 (*continued*)

ID	adj.P.Val	P.Value	t	B	logFC	SEQUENCE
ASCRP3006838	0.018	0.00004741	9.388032	2.6999	1.758564	CTGTGTGGTGCGAGTAACTGTACAGTGTGATCACTTACTCCAGTCGTCATGTCTACAATA
ASCRP3009307	0.1206	0.00781549	3.770276	-2.4048	1.757309	GCTTTGGTGGCAGCCGTGGTGGTGGTTTCGGTGGGAATGACAACTTCGGTCGTGGAGGAA
ASCRP3011563	0.3196	0.06295095	2.234346	-4.5382	1.745266	TCTCAAAATCCATTCCTTTAAAAAATAAATCTGATGCAGATGTGTAGGCGGGAGCAGGGC
ASCRP3008380	0.0552	0.00168586	5.098631	-0.8132	1.738928	GAGGTGTGCTTTGTGTGAAAGGTGAGCAATAAAGTATCTGTTAAGTTCGTGTTGATGGGC
ASCRP3011719	0.0208	0.00009866	8.330483	2.0173	1.738267	TCTTTCTTATTCAGGTGTGTGTAACTGGTGTGTGCACCGTTTCGACCATCACTGTGTTTG
ASCRP3010469	0.0661	0.00246982	4.746316	-1.2079	1.734672	GTTTCTGGTGTGTGTTCTAGGTCAGTGGCTTCAAAGACTCCAGTTGGATTCATTGGACTG
ASCRP3007143	0.0535	0.00145668	5.237739	-0.6627	1.718509	CTTGTGCCTTGGTGTGTGTTATCGGAGGTTTCATTCCTGGAAAATCCAGTGTCTATGAAA
ASCRP3008446	0.0279	0.00034843	6.743406	0.7884	1.708975	GAGTTGATCAGTGTGGTGTTGGAGCCAGTGCACAAGTGCAGGGACTTGAGATGGGAGTAC
ASCRP3008559	0.0542	0.00157852	5.16096	-0.7454	1.685167	GATCGGTGTGGACTTTTCCGGGGTGGTGTGGTCGGTTAGGAAGAAATTTGGAGTGTGCGT
ASCRP3002172	0.0208	0.00015213	7.7546	1.6024	1.682398	AGCTTGAGTGGGAGTGTGTGAGCGTGAGCGAGCGGGTGTGTATGTACGAGTGTGCACGTG
ASCRP3003070	0.3355	0.07014861	2.159026	-4.6449	1.682132	ATGGAGGGCCAGTTATAACAGTGCAGAATGCCACCCAGAGGATGTTTGAAATTGACTATA
ASCRP3000125	0.0277	0.00031557	6.858393	0.8869	1.675352	AAACAGTGTGGTGGTATCCTTACAATCATCCTGCTTCTTGTACATCACTGACGTCTGCTC
ASCRP3013256	0.3826	0.09513604	1.94737	-4.9415	1.655404	TTGGTTGGCTTGTCAGATGAACTGGCTAAACTGGATGCATTTGTAGAAGGAATCTCTCTT
ASCRP3007899	0.0581	0.00186406	5.004382	-0.9169	1.625438	GACCATCAGTCATGCTCTGTGGGTGAGAGAGCCAGCCCAGAAAGGACTGTGCGGAGATTG
ASCRP3013138	0.1673	0.01532347	3.249468	-3.103	1.62009	TTGAAAAAAAGATACTGTGTTTTTTCACTTGCCACCCAGAAATGGAAATGGAGCCACAGT
ASCRP3010410	0.0673	0.00267625	4.674232	-1.2911	1.610373	GTTGCATCAGTGTGGTTGTGGTTTAGGAGGGGGGCATTCCAAAGGCAGGTGAATAAATGG
ASCRP3010304	0.0223	0.00018421	7.510944	1.4166	1.610102	GTGTGTGGCCAGTCATTTACCACCAATGGGAACATGCACAGATACTTTCGAGTCCTTCTC
ASCRP3006170	0.051	0.00122396	5.406726	-0.4838	1.599071	CTCATTCATGTGTGGTGTTGCGGATGGAGAGGGTTTTCTGAGTATCTGGCAAGTTAACCA
ASCRP3009014	0.0195	0.00005633	9.129542	2.5419	1.586236	GCCAATTTTACATTTAAGGTGAGTGTCTGGGTGGTGCTTTATACTGGAAGGAACTTGCTG
ASCRP3008436	0.3118	0.05880218	2.281857	-4.4706	1.575916	GAGTTATTACAGTTTCAGGATTGGCGGGCTTGGTTTCAGCGAGAAAAGATGGGAAAACTG
ASCRP3011392	0.1072	0.0063432	3.938477	-2.1878	1.566593	TCCCTGTGGTGGAGTTTTTGACACTTTTGTTCAAGTACACATTTCATCAGGTGACTTACT
ASCRP3000424	0.3099	0.05794148	2.292142	-4.456	1.561817	AACCACTCTGGAATACTTGCTGGCTGGGGCAGATATCATTGAAACAAATACTTTTAGCAG
ASCRP3005757	0.0758	0.00346044	4.447849	-1.5578	1.556615	CGTGTGTGGGGTCGAGCTTCCTGATAACGAGGCTGTGGAGCAGCACAGCCTCCTCTATTG
ASCRP3010723	0.0955	0.00503038	4.129548	-1.9466	1.547208	TACCACAGCTGCCTTTGTGTGTTTGTGTCAATAAAAAGCCAAACCCTGGGCTCGCCCGGC
ASCRP3007287	0.3663	0.08544204	2.022024	-4.8376	1.546151	GAAAAATATATGAGCTGGCTGGGAAAATGAAAGGATGGCCTGGTGGGAATCCAACAATTA
ASCRP3010298	0.0628	0.00217796	4.860596	-1.0777	1.543463	GTGTGGACATGTGGGCTGTTGGCTGTATATTAGCAGAGTTACTTCTAAGGGTTATAATAA
ASCRP3013460	0.3716	0.08939674	1.9906	-4.8814	1.541288	TTTGCTGGCTGGGCTTTTCCAGTGTCAGAAAGAAGGTAGAGTGGAACCCCCAGCTATTAG
ASCRP3008107	0.3372	0.07083976	2.15221	-4.6546	1.538981	GAGACACATCCAGGCCAGCCTTTATTATTGCCATATAAGCCTTCTGGTAGTACCAAGATG
ASCRP3005597	0.3208	0.06334755	2.229973	-4.5444	1.527185	CGAGATGGGGCCTGGCGGGCTTTGGGCTTTACTATATATGGATGGATCCATAAACACATG
ASCRP3002496	0.0657	0.002416	4.766216	-1.1851	1.525055	AGTTAGGGCCAAGCTTCATGAGTTCAGAGGTCTTTGAATAGTGTGTGTTTTGTTTTTGGT
ASCRP3009639	0.4327	0.12197664	1.774271	-5.1783	1.520785	GGCTGCTGGCTTCTTTGTATAGCATCCATGAGTATGTTTTCTGATTTCCTGCAGTCTTTT
ASCRP3012667	0.4148	0.11250833	1.830661	-5.1018	1.519275	TGTGGCTTATGGCTGGATTATACTAAAACATACAACTTGGAACTGCAGTTGGCTTTTTGC
ASCRP3004615	0.3355	0.06994973	2.161	-4.6421	1.502339	CATCCAAAGGGCTGTGGAGAGGACTCAAAGCCACCCGTCATCTCGTTACAAAAGCTCATC
ASCRP3011094	0.3316	0.06730062	2.187847	-4.6041	1.489746	TCAAAATCCATTCCTTTAAAAAATAAATCTGATGCAGATGTGTAGGGAGAGCCTGGGGCC

Table S2 (*continued*)

Table S2 (*continued*)

ID	adj.P.Val	P.Value	t	B	logFC	SEQUENCE
ASCRP3003420	0.0208	0.000132	7.939592	1.7392	1.481835	CAAAATTCTGCTGGTGAGAGTGTGTGAAGGTTTGTTTTCTGCCCTAGACAGTCATTCAAA
ASCRP3005985	0.4205	0.1151874	1.814252	-5.1242	1.478179	CTATATTCCCTTTCCAGAAGATGATTCCAACGCCACCAATTCCAACCTGGTTCCAACTAT
ASCRP3011351	0.018	0.00004283	9.543626	2.7925	1.467179	TCCAGGGGATAGTGGTGTGGATCAGTTGGTAGAAATAATCAAGTTGTATATGTATCAGCT
ASCRP3001452	0.5227	0.19019845	1.460359	-5.5862	1.465313	ACGCCAAGCCAAGCAAATTGTTTCATCAGCAAAGGAACTATAGATTTAGCTTATTGTGAC
ASCRP3009533	0.0591	0.00197386	4.951196	-0.976	1.464261	GGATTACAATTCTTCTAATGCCTTGTAGCTGCTGCTGGTGGTGACAATGTCAAATAACGG
ASCRP3009348	0.3856	0.09669718	1.936058	-4.9571	1.45978	GGAACTCTTCAGCCAAGCCATATCTAACAGAACTATCTTCAACTTTTCAGGCTGCAATAA
ASCRP3008429	0.3778	0.09292664	1.963698	-4.9188	1.455657	GAGTGGCCTTGGCTGGGGAGTATGGAGCAGTCACTTACAGGCAATTTTTACCCAGAAAAG
ASCRP3010242	0.3133	0.05962647	2.27215	-4.4844	1.454795	GTGGCTGAAGAAGTGCTGGCCGGGATGAATGTCTACTCCTCTGAATTTGAAAACATCAAG
ASCRP3008718	0.3957	0.10149183	1.902409	-5.0036	1.448042	GATGTCTGGAATGGCTGGTCTTTTTAGCATCTCTGGCAAGATATGGTTACGCCCCATGGT
ASCRP3011137	0.0208	0.00015125	7.762101	1.608	1.446225	TCAAGATAGATATTATAGCAGGTTGTGTGTTGGATTTGACATAGATGAAGACGCATTGGA
ASCRP3010724	0.1259	0.00848486	3.704988	-2.4902	1.438587	TACCACAGCTGCCTTTGTGTGTTTGTGTCAATAAAAAGCCAAACCCTGGGTCCTGGTGTC
ASCRP3000445	0.2656	0.03935417	2.563681	-4.0683	1.426812	AACCTGAGGAGAGAATGGCATGCCAGATGATCTCAATGCCACCCACCAACACTGTGTTTT
ASCRP3007667	0.1862	0.01904351	3.087549	-3.3272	1.423974	GAAGTGTTTGGTGAGATTGAGGAGTGCGAGGTGCTGACAAGAAATAGGAGGACTCACCCC
ASCRP3008203	0.0352	0.00052885	6.275189	0.3703	1.417457	GAGATTGAATGTGCCACTTGCATTCACAAGAGATGGGCTCTGTGGTCTGTGGAATGAAAT
ASCRP3004481	0.1206	0.00797514	3.754162	-2.4258	1.415975	CAGTGTGTCTGGTCTTATGAGAACATGGTCCAAGACAATTCCTGGGAAAGTTCAGTTCTT
ASCRP3008112	0.0226	0.00019047	7.469053	1.3841	1.412543	GAGACATAAGTCCCATGAGGATCCCAGAGTTGTGGCGGCTGGTGTGTTCATCTTTTGCTA
ASCRP3012915	0.0484	0.00093142	5.679333	-0.2041	1.412305	TTCAACTTCACCACTCAAGATGTATGGTCTGCTGGCTGTGTGTTGGCTGAGCTGTTACTA
ASCRP3003196	0.3355	0.06984069	2.162084	-4.6406	1.402895	ATTAGTTGGGAAGAAGGAATGAAGGCTTGGGTGGCAAATTTTGAAAGACCTCGAATGAAT
ASCRP3009275	0.5067	0.17508738	1.519544	-5.5119	1.400806	GCTGTGCCAAGCCACCAGGGAAGCTTCTGCATGCTGTGTGTCATGCAGAACCACATTGTC
ASCRP3012226	0.4618	0.14126982	1.671371	-5.3155	1.395519	TGCTGGCTGGTGCAATGCTTGCCTTGGGACTAATGACATGCTTGTCAGGAGTCGGGGCTG
ASCRP3007454	0.052	0.00127539	5.366441	-0.526	1.388058	GAACAGCAAGCCTGTGCAGGAGACATGGCGGACGCAGCATCTCCGTGCTCTGTGGTAAAC
ASCRP3010438	0.0674	0.00278829	4.637659	-1.3336	1.380768	GTTGTGCCTGTTTGTGAGTTTGGTAAAAGTAGTGGCATTCTGTTATTGGACAGCTGTCAT
ASCRP3007536	0.0657	0.00240994	4.768488	-1.1825	1.379516	GAAGAATCTCATCTTGTATAAAGACAGACCAAGGGGTGCTGAGTGTGTGTTGCTGTTCAT
ASCRP3013581	0.3375	0.07108032	2.149854	-4.6579	1.373231	TTTTGTTGCTGGTGAGGCTGGTTGACCATCGAGTGAACTTCGACCACTTCCAGATCCTTC
ASCRP3008965	0.3271	0.06556508	2.206023	-4.5784	1.360992	GCAGTGGAGAAAGCCATCAAGAAATTTGGAGGAGGCTGGCAGGATGTACAGTTTTTATCA
ASCRP3010303	0.0277	0.00031675	6.854046	0.8832	1.357718	GTGTGTGGAAAGGACCCACTCTTCTGTTTGTAAAGGTGACCCAAGGGAAAGAAGAAACTC
ASCRP3009875	0.1374	0.01039801	3.545593	-2.7014	1.349636	GTACATCTACATGCATTTTGGGGAGGTCCCTGAGTGCCAGAGGTGGTGGTGTTGCTTATC
ASCRP3011773	0.0279	0.00035062	6.736195	0.7822	1.346934	TGAAGAAAGAGGTTTTATGTGCCAAGTGGGAAGAGATCAGTGGTGTGGATGAACATTACA
ASCRP3008066	0.0347	0.00049075	6.357212	0.4455	1.341796	GAGAACAAGAATAAAACAATAACTGTGTGTGTTCTGGCTGAGATCCGAAAGCCCCCAATG
ASCRP3001315	0.2251	0.02828172	2.799288	-3.7327	1.340719	ACCATTCCCGTTCTTTGGGGTGACTTTCAAGATGGACTCTACTCTAACAGCAAGTGAAAT
ASCRP3002566	0.018	0.00004456	9.482894	2.7566	1.338792	ATAACATTAAGAGTATTGCTTTGTAGTGTGTGTATCTGCACACCTGGCGCCTAAGTGTGG
ASCRP3013228	0.0279	0.00034678	6.748867	0.7931	1.33393	TTGGAGTACCGTTCGGGTACTTCCTATTTAACAGACATTGTGTGGTGGGCTGGCACAATC
ASCRP3010241	0.3343	0.06868898	2.173646	-4.6242	1.333183	GTGGCTGAAACAAAGTGGTCCAGCAACACTCGCCTGCAGCAAGCCACCCAGAGCTTCACG
ASCRP3002476	0.2284	0.02966892	2.764878	-3.7816	1.323873	AGTGGGAGATTTGGAACAGCTTTGAGAAGAGCAAGGTGGTGGTTATTTAATGGGTATTTG

Table S2 (*continued*)

Table S2 (*continued*)

ID	adj.P.Val	P.Value	t	B	logFC	SEQUENCE
ASCRP3007900	0.0674	0.00278355	4.639173	-1.3319	1.321098	GACCATCAGTGAAGAAGAAGGTAACGGCGACTGTGACTGTGGTGAATGTGTGTGCAGGAG
ASCRP3003648	0.5169	0.18425998	1.483085	-5.5578	1.31624	CAAGCCACAAGAGACGTCATAATCAAGGAAACACACCCTGAAAACCAAACCTTGAGAAAG
ASCRP3001629	0.0179	0.00000988	12.060455	4.0608	1.315285	ACTTATGTGAACCTGAGCAGTTTGTGGTTGTGTGTTGAAAAAGAGTTTACCGACCACCAAG
ASCRP3003254	0.0635	0.00223291	4.837818	-1.1035	1.315255	ATTCTGTGGTGGATCCAGTGGAAAAGAAAATGGAACTTTGTTCTACCAATCCACCCGTGG
ASCRP3012742	0.05	0.00110248	5.509951	-0.3766	1.314531	TGTTTGGTGCAGAAGGTTGCAGTGAGAGCAGATGCTGGCAAGAAGCACTTACCAGACAAG
ASCRP3002608	0.3492	0.07674424	2.096584	-4.733	1.310987	ATACAGTCTAAATTGCAGGAGGCAGAAAAGGCTGGCATGGTTCATTTGTTGGATTTCCTA
ASCRP3009369	0.0344	0.00045409	6.443234	0.5236	1.310955	GGAAGGTCAGGCCTGCATGTATCTTAGTGTGTCTGCTGGTGTGAGTGTGATTTGAAGATG
ASCRP3011873	0.0208	0.00012098	8.054956	1.8228	1.309052	TGACTATTGAAGGTGGTCGTGTGATGGTAACAGATGCTGACAGGTCAATACTATCTCCAG
ASCRP3003771	0.0891	0.00453165	4.217098	-1.838	1.305109	CAATGTGCTCTGGGACCTGGTTGACAGGATAGGGGCACCCTCATCCAGCATCTGAAGGAG
ASCRP3011583	0.3716	0.08922055	1.99197	-4.8795	1.301369	TCTCCCGATCTGTGGCTGGCTCCTATGATAATGAAGGTACTTTAATTATCGGACTACCAG
ASCRP3000051	0.0195	0.00006941	8.824376	2.3481	1.298583	AAAACCACACCGACTTCAAGGACAAGATGAAGATGTGTGTGTCTTTAAGTGCTCAGTGTC
ASCRP3011550	0.5806	0.24161809	1.286592	-5.795	1.296859	TCTAGCCAGCCAGCTGAAACGGACTCCATGATAAGCAACGATGTGCTGAGCTGAAGAAAG
ASCRP3002845	0.1206	0.00780188	3.771666	-2.403	1.289192	ATCCTTGATTTGTCATCAGAGATGTCATACTGACTTGGAGTGTGTGTGGGTGACCAAATC
ASCRP3007869	0.0955	0.00507319	4.122484	-1.9554	1.285533	GACATGGTGGTGGTCGAAGTCAGCAGACACTAGACATGAGCCTTTGAATACATCTTTATC
ASCRP3010073	0.0879	0.00444635	4.233137	-1.8183	1.281852	GTCTCATAAGCTTGCATTCACAAGAGATGGGCTCTGTGGTCTGTGGAATGAAATGGTTAA
ASCRP3012795	0.291	0.05040929	2.389479	-4.3172	1.277003	TTAATAAATTGCCTTCATGTAAACTGTTTCAAGGAAACCATCTGCCGTGTGACTGGTGGG
ASCRP3002320	0.2499	0.03556705	2.63541	-3.9659	1.270123	AGGGCTGGCCAACTTCTGCTACAGACGACTCAGAGAGATTAAACAGATTCTAGAAAATGA
ASCRP3010582	0.0661	0.00250609	4.733172	-1.223	1.261236	TAACCAGAAAGAATGCAGCTGGGATTTTGCTACTTGATAATGTGTGTGGGGTCTAGAAGT
ASCRP3003314	0.3764	0.09235803	1.967962	-4.9129	1.257673	ATTTAAGATTGTGGGCTTGGCTGCTTTCCTGCCAACCAACCTCGGTGCAGGATCAGCATT
ASCRP3004233	0.0179	0.00001706	11.060188	3.6041	1.23708	CAGCAAGACTGTGTGTGGACCAGTGGCTAAAAATGCCAGGAGAATATTAAACGTAAAGAC
ASCRP3007675	0.0617	0.0021187	4.885889	-1.0492	1.23707	GAAGTTGTGTGTTGTGCAGTCAGTAAAATCCTCCCACTGCCTCCGGGTCTTGCCCCAGAA
ASCRP3010290	0.1396	0.01123109	3.485944	-2.7813	1.236408	GTGTGAGCATGTATGTGTATATGTGAGCAGCTGTGCACGTATGATGTCAGTGGGTGTCAG
ASCRP3000044	0.0232	0.00020435	7.381417	1.3153	1.230818	AAAACAGTCGGTGTGTGCTGAGCAAATGGAAGAACAAATATGTCTGTCAGAAAACCATGA
ASCRP3006891	0.3063	0.05674437	2.30671	-4.4352	1.230735	CTTACGAGCTGGTCCTGGCTGATGGCAGCTTTGTGCGATGCACTCCGATTGTCCGTGTGG
ASCRP3010255	0.5165	0.18381603	1.484811	-5.5557	1.228119	GTGGGTGGCTTTGGACTGGTCTGAGGTTAAAAAATGGCCATACTTTAGTAACTAATCAGC
ASCRP3010467	0.1428	0.01155111	3.464301	-2.8105	1.223524	GTTTCTCAATAAGCAAAAAGAACCATCTGCTGCAGAATCCCAGGGGAAAGGCAGCATCTC
ASCRP3001970	0.018	0.00003737	9.756047	2.916	1.222876	AGATTCCACATAGACAAGGGACAGCAGTGTGGACTGTTGGCTGGTAAAGTGTGTGCAATG
ASCRP3005925	0.3316	0.06753086	2.185471	-4.6075	1.221288	CTACTGTGTGCCACCCCAAGAAGGCCAGCGAGAGATGGAGCTACCGTGTCCAGGATGAAG
ASCRP3002278	0.0552	0.00168437	5.099468	-0.8123	1.216644	AGGCAGAAAAAATAAAGAGGGTTGATTTCTTTATTCCAGGAGTCTCTGTGGTTGGTGGGT
ASCRP3010254	0.1206	0.00797174	3.754501	-2.4254	1.216385	GTGGGGGCGTGTGGATTAAACTTCATTGACTTGATGGTGCGACAAGGGAATATTGACAAC
ASCRP3010305	0.0208	0.00014936	7.778396	1.6202	1.212397	GTGTGTGTGAGTGCACTTGTGTGTGGGTGACTAAGTGGATGCATGTGTGCCCCTGCACTC
ASCRP3006072	0.0179	0.00001243	11.630658	3.8714	1.205621	CTCACACATCAATGCTTATGCCTGTCTGGTGTGTGGCAAGTACTTTCAAGCAAAGAATGG
ASCRP3007880	0.1907	0.02071376	3.025619	-3.4137	1.200455	GACATTTTGGATCCAAGTTTGTTACTGCAGTGGCTACAGGTTGGCTGGATATTTACAGAC
ASCRP3004461	0.0228	0.00019557	7.436005	1.3582	1.200382	CAGTGCATCTTCTAGCTGAAAATGTGTGTCTGACATGCAAGCTCAGTGGGGCAGAGACCC

Table S2 (*continued*)

Table S2 (*continued*)

ID	adj.P.Val	P.Value	t	B	logFC	SEQUENCE
ASCRP3002006	0.3186	0.06250849	2.239258	-4.5312	1.190954	AGCAATCAGCTGGCCTGGTTTGATACTGACCTGTAAATCATCCTTTAGGGTATTTGAAGT
ASCRP3004689	0.2836	0.04653958	2.4455	-4.2371	1.189943	CATGAAAATCACAAAATTGGCACTCAGTGACCATCAGGCTGGCTGTGTGCGGCAGCTTCC
ASCRP3000710	0.0208	0.00014115	7.851798	1.6747	1.188934	AAGTACCAGCAGAAGGTGGTCGTGTGATGGTAACAGATGCTGACAGGTCAATACTATCTC
ASCRP3006376	0.0526	0.00135352	5.308608	-0.5871	1.187439	CTCTGCGTGTGCTGTGGTTTCCACTAAACACTAAAATGAGGAAAGAGGAATCAGAAATGC
ASCRP3011446	0.3704	0.08852891	1.997375	-4.872	1.187301	TCCTGGTGATATTGTAGAAATTGCTGGTTTTGGCTTGGTTTGAAGAAGGTGAAGAAACAA
ASCRP3009488	0.112	0.00688217	3.872346	-2.2726	1.186447	GGAGTAGCTGCTGAGGTTGGTGTAAACGGGAGGTAGCTGATGGTGGTCGTCGGGTACGAG
ASCRP3006644	0.1777	0.01715518	3.165009	-3.2196	1.183953	CTGCTGTGGTGGAAAGGAACACATTAATGGGATTCGGGGAAACTGCAAGGCTTATTTCAG
ASCRP3007421	0.321	0.06349571	2.228346	-4.5467	1.179135	GAAATGCTAGGAGTTGAGCCTGGCTGGGTGGAAGGTGTGAGTTTGCCAGCATAGATCAAG
ASCRP3008637	0.2974	0.05240352	2.362321	-4.3559	1.177872	GATGATGAAGAAGACCTGCTGGATGGCTGGGAGTGTCTGCTGATCACTTGGAGTGCTGTC
ASCRP3005060	0.1767	0.01663886	3.187793	-3.188	1.169858	CCAGGATCTGGCTGGTGGAGGAAGTGAAGGAGCTGTGTGATGGCCTGGAGTTAGAAAATG
ASCRP3011358	0.2055	0.02401852	2.917461	-3.5656	1.166647	TCCATGATGAGGTGGCTGGGATCGTTGGCAGAGCGGACGTGTTAGCGTGTCTGCTGTTTC
ASCRP3011544	0.0179	0.000016	11.173151	3.6586	1.162077	TCTACTGGTCTGGGATCTTGTGTGTGATAATGCCTGGAAGGTCCATATCGCTAAGTTCTC
ASCRP3006295	0.0963	0.0052121	4.100009	-1.9835	1.161291	CTCGGATAAGTGTTGCTGTGGATGTATGGTCGACGCTGGCTGATTTCTGTAACATACTGA
ASCRP3006867	0.314	0.06003455	2.267395	-4.4912	1.143492	CTGTTTGGCCAGGCTGGACTGGCGACATCTAGACTAAGAGAAAGAGGCTGTGATGGTTGC
ASCRP3006528	0.4558	0.13754742	1.690132	-5.2907	1.141389	CTGAGGAAGTCTTTGAGTGGCTGGCGTGGCTCACCGATTCCACAGTACTTGCGGCAAGAA
ASCRP3002530	0.0277	0.00032001	6.84211	0.8731	1.140874	AGTTTTACCATTCTGTATGGTGTTCTGTGTTTTTTTGCCAGTTGTGCTCCTGGTTCACAT
ASCRP3012236	0.0875	0.0043983	4.242324	-1.807	1.13573	TGCTTAACTTAATGTAGTGAAATAAAGCAGACAAAGCTTGAGTGGTGGTGCCTCCCAAAG
ASCRP3010329	0.3718	0.09013689	1.984873	-4.8894	1.134107	GTTACACAGGGTTGCGAACACACCTCGGCTTGGCTACTAATGAGGGTTACGGGTAAATTC
ASCRP3002149	0.3799	0.0938775	1.956624	-4.9287	1.132869	AGCTGAGGACCCAGATATGTATCAATGAAGTCAAGGCATCCATTCCTTCAACATGCTTTA
ASCRP3009532	0.0208	0.00009619	8.365296	2.0413	1.126389	GGATGTGTGGGGAGAGTTGAATTTCAAAATAATTACTCTACAAATAGTAGAGTGATGCCT
ASCRP3005645	0.2947	0.05130267	2.377178	-4.3347	1.124923	CGCAGGCTGGGCTGATAAAATTCATGGGATGACCATTCCTGTAGATCTTTATAAACAACG
ASCRP3007488	0.1072	0.00629443	3.944764	-2.1798	1.11761	GAACGGGGTGCTAAGCATGAGGCCTGGCTGCTGCTACCATTCTTCAAGAGCACTGCTTCC
ASCRP3006812	0.0652	0.00236225	4.786592	-1.1618	1.115039	CTGTGCGTGTGGACTTCTACAATGCAGACGAGCTCAAGATGGAAAGCCCGTGTCTCTGTC
ASCRP3006132	0.0674	0.00270385	4.665067	-1.3017	1.109887	CTCAGTGCCAGAGAACCGAGCATCCAGTCATCTCCTATAAAGTGTTGGTGTGTGAGACTT
ASCRP3008448	0.0367	0.00058325	6.168983	0.2714	1.108216	GAGTTTCTCTTGAGGGCAATAAAAGTTGTCATGGTGTGTACGTGGGGAGCTGCTGTTGAC
ASCRP3008773	0.2955	0.05180503	2.370358	-4.3444	1.107415	GATTGATTCTGTGTGTGCCTCTGACAGCCCTGATAGGCAGTAGACAGCAGGGACTCCCTG
ASCRP3006332	0.1428	0.01155579	3.463988	-2.8109	1.102709	CTCTCAGTGGGGCATCAACCATTCCACCGAGATACTTTCCACTTTCTAAGGGAGGAAAAG
ASCRP3007295	0.2346	0.03106992	2.731811	-3.8286	1.093922	GAAAACTTCAAGTACTGAGTCATGCAGGGCCTGGTCTGCTTGAATCCTGTGTGTGTGCCG
ASCRP3011929	0.245	0.03353141	2.677356	-3.9061	1.089448	TGAGTCACCAGTTAACTATGGTAGCCCACCCAGCATTGGTGAAGTATTACAGACACTTAG
ASCRP3005771	0.4211	0.11586085	1.810185	-5.1297	1.087184	CGTTTCAAAAGCCAAGCCAGTTAACGCGACACATTAGGATACACACAGATGGAGTTTTAA
ASCRP3000719	0.2274	0.02926658	2.77468	-3.7677	1.086147	AAGTCAGAGAGGTACTTCGTACTGGATTTCGAGGCTGGCATCCTGCAGTATTTTGTGAAT
ASCRP3010613	0.0539	0.00155982	5.172306	-0.7331	1.08437	TAAGTGAGAAGGGTGTGGTGCAATTATTTAATGCTGTTCAGAAACATCAAAAGAATGTTG
ASCRP3006087	0.0391	0.00066383	6.030655	0.1405	1.080441	CTCACTGAAACAGCAAAACAGACATTGCTACAAGTGGTTGGTGTGGTCTCTGTGGCTGTG
ASCRP3011687	0.2484	0.03507149	2.645385	-3.9517	1.078937	TCTTCCAATGAGCCCATTCCAGATGATGGGATTTATTGGCAGGCCAACCTTGACAGATTC

Table S2 (*continued*)

Table S2 (*continued*)

ID	adj.P.Val	P.Value	t	B	logFC	SEQUENCE
ASCRP3002315	0.0277	0.00032733	6.815741	0.8506	1.074089	AGGGATGGTACAACAGATGCAGTCTGTGTGCTCTGATTGTAATGGAGAAGAGTATCTTTA
ASCRP3002862	0.0674	0.00281834	4.628131	-1.3447	1.07221	ATCGGTGGTGTGAAAACATTGGAAGAGCCCATAAGAGTAATAATATAATGACGTTCATGT
ASCRP3009332	0.2948	0.05144643	2.375219	-4.3375	1.070656	GGAAAGTGGCTGGATTGGACAAGCAGGCAAAGCTGAGGGATATGTGGTGCCTGTCATAAG
ASCRP3000341	0.3075	0.05709645	2.302393	-4.4414	1.069023	AAATTGCAGTCAATGCATTATGGCCTAAAACAGGAGGCTGGCAGGATGTACAGTTTTTAT
ASCRP3009644	0.1072	0.00634276	3.938535	-2.1877	1.062291	GGCTGGGCAGGGTTTTGTCCACCTTGTGTCTGTAGCATCTAGGATGGTGTGTGTGTGTGT
ASCRP3005738	0.1862	0.01905274	3.087191	-3.3277	1.060478	CGTCTGTGTGAGCGGTTTAATGAAAGAAATCCACCTGAACTTATAGGAAGATTCTTACCT
ASCRP3009641	0.373	0.09093382	1.978758	-4.8979	1.056464	GGCTGGAGTGGTTCCTTAAATGTCGAAGAAGGGAAGAAGAAGGAAATACTTGCAAAACAC
ASCRP3013141	0.2368	0.03165228	2.718527	-3.8475	1.051723	TTGAAAAATCACATGAAGGAAGGAAAACAGAAATAACTTGCTGGCTTGTCTGGAGTCACA
ASCRP3001509	0.0509	0.00118908	5.43514	-0.4541	1.049465	ACTCACCTGCTAATGTTGATGCTGCGTGAAGGTGGTGTTTTTAAGGCTCATCTTACTTTC
ASCRP3002996	0.1442	0.0118574	3.444188	-2.8376	1.044092	ATGATGCCAATGGTGATGTGGATGTGGAAGAAAGTGATGAGAGTTTTGCCGAATTGACAA
ASCRP3005164	0.3622	0.08331899	2.039497	-4.8132	1.043204	CCCAGCCATCAGTTATTCAGTCTCCACAAGTCCAAACAGTTCAGGTAACTAAATGACCAT
ASCRP3009345	0.5073	0.17576181	1.516804	-5.5154	1.043025	GGAACTAACAGATCTTAAATTACAGTTGGAAAAGGCCACCCAGCCCTGTAAGACCAGTAA
ASCRP3005130	0.4108	0.1100522	1.846043	-5.0809	1.040085	CCATTCCAGGACTTGTGGACAGTACCTGCAGTACGTGGATCATTCATGTGAATGGCTTTC
ASCRP3007802	0.3572	0.08056538	2.062836	-4.7804	1.03952	GACAAGTTCATTCCATTATTAGACGTTCCCTGCCAGCAACACTACCACAGCTTATGCAAG
ASCRP3006814	0.1385	0.01085543	3.512223	-2.746	1.036614	CTGTGCTTGGGTGTGCAAAGGTAAGCGAATAAAGGAACTGGCTCAGCCTGTAGTGTTTAC
ASCRP3000870	0.5012	0.16990794	1.540917	-5.4848	1.033698	AATGAGCTTGCATTCCAGCCTCCCATTTCCAATCATCCTGGTCAGCCTGCCAGTATACTG
ASCRP3012682	0.2261	0.02872566	2.788085	-3.7486	1.029728	TGTGTGGCTCTGTATGACTGTTGCTGAAATATAAAGCCCTGCAACCTGGCAGCCGCCCTC
ASCRP3009190	0.0484	0.0009222	5.689436	-0.194	1.028342	GCTATTGTCATTAAAGAAACCAAAGGTGTCTGCAGTGCTGTGTGATGATGACATCATGCT
ASCRP3000759	0.1327	0.00966035	3.602931	-2.625	1.026102	AATAAAAATTTATGGTCCAAGGGAGTGGTGGTGACCAAGGCGGCCATGATTGTGAACCAG
ASCRP3013498	0.4902	0.16134952	1.577596	-5.4378	1.024736	TTTGTTACCTTCCGAGCCACCCGAAAACCTCTAGTACAGACAACCCCAAGGGTCGAGCAC
ASCRP3005749	0.0344	0.00047605	6.390789	0.4761	1.02301	CGTGCTGTCGTGCAGGAGAAGGAAAGGAGGCTGAAGGGTACATCCGGGAAGGCTTCCTGG
ASCRP3007053	0.2228	0.02759749	2.816925	-3.7077	1.022729	CTTCTGTGCTTGGCTCAGGAAAAGCTGGAACGGGTGATCCTAGGGAGTGAGGCTGCTCAG
ASCRP3008589	0.0208	0.00008764	8.494247	2.1294	1.015729	GATCTTCCAGAGAAAGGACCAGGGAGTGTGAGGAAGAGGCTGTCTGTGTCATTATGTGTG
ASCRP3006589	0.3049	0.05638671	2.311124	-4.4289	1.015579	CTGCATGCTCTTGGCTGGAAGGTTGCACTCCAGGACTTGCAGACGAACTCCAAGATTGGG
ASCRP3000112	0.0268	0.00026433	7.067978	1.0624	1.01071	AAACAAATTGGCAGTATAAATTTAATGTGTTGTTTTCAAGTGTGTCATGTGTCCAGATGC
ASCRP3005927	0.05	0.00113729	5.479115	-0.4084	1.010658	CTACTTATCAGGTGCTGTGCTGGTGATATGGGGTGAAAGTCCCATGAAGACACATATATG
ASCRP3011357	0.1111	0.00673174	3.890214	-2.2496	1.006711	TCCATCTGCTGCAAGGAAGTTTGTAGATGAAGGAATTAAAACACTAGAAGAAAAGCAGCA
ASCRP3013015	0.05	0.00110937	5.503767	-0.383	1.006197	TTCCGGTGAAATAAATGGTTTTTCAACTTAGGGTAGTGGGATGTGTGTGGGCTGAAATTC
ASCRP3002158	0.4702	0.1469808	1.643482	-5.3522	1.005072	AGCTGGCTTGGCTGTTCCCTGGATGGGCAATAAAGAAAGTGCTGCATCCCCCGCGGCAGC
ASCRP3001872	0.4476	0.13218908	1.718006	-5.2537	1.003735	AGAGCCATTCCTTTTGGAACAATGATGATGTGATGCCAGCCACTTACTGTGAAATTGATT